TRIM6 interacts with Myc and maintains the pluripotency of mouse embryonic stem cells

Tomonobu Sato[1,2], Fumihiko Okumura[1], Tadashi Ariga[2] and Shigetsugu Hatakeyama[1,*]

[1]Department of Biochemistry, Hokkaido University Graduate School of Medicine, Kita15, Nishi7, Kita-ku, Sapporo, Hokkaido 060-8638, Japan
[2]Department of Pediatrics, Hokkaido University Graduate School of Medicine, Kita15, Nishi7, Kita-ku, Sapporo, Hokkaido 060-8638, Japan
*Author for correspondence (hatas@med.hokudai.ac.jp)

Accepted 2 November 2011
Journal of Cell Science 125, 1544–1555

doi: 10.1242/jcs.095273

Summary

The proto-oncogene product Myc is a master regulator of cell proliferation through its specific binding to the E-box motif in genomic DNA. It has been reported that Myc has an important role in the proliferation and maintenance of the pluripotency of embryonic stem (ES) cells and that the transcriptional activity of Myc is regulated by several post-translational modifications, including ubiquitination. In this study, we showed that tripartite motif containing 6 (TRIM6), one of the TRIM family ubiquitin ligases, was selectively expressed in ES cells and interacted with Myc followed by attenuation of the transcriptional activity of Myc. Knockdown of TRIM6 in ES cells enhanced the transcriptional activity of Myc and repressed expression of NANOG, resulting in the promotion of ES cell differentiation. These findings indicate that TRIM6 regulates the transcriptional activity of Myc during the maintenance of ES cell pluripotency, suggesting that TRIM6 functions as a novel regulator for Myc-mediated transcription in ES cells.

Key words: ES cell, NANOG, Myc, TRIM6, Ubiquitin

Introduction

The ubiquitin-mediated proteolytic pathway has a crucial role in the elimination of short-lived regulatory proteins (Peters, 1998) and in the quality control of proteins, including those that contribute to cellular signaling, the cell cycle, organelle biogenesis, secretion, DNA repair and morphogenesis (Hershko and Ciechanover, 1998). The system responsible for the conjugation of ubiquitin to the target protein comprises several components that act in concert (Hershko and Ciechanover, 1992; Scheffner et al., 1995), including a ubiquitin-activating enzyme (E1), a ubiquitin-conjugating enzyme (E2) and a ubiquitin ligase (E3). The resulting covalent ubiquitin ligation induces the formation of polyubiquitinated conjugates that are immediately detected and degraded by the 26S proteasome. E3 is thought to be the component of the ubiquitin conjugation system that is most directly responsible for substrate recognition (Hershko et al., 1983; Huibregtse et al., 1995; Scheffner et al., 1995). E3 ubiquitin ligases have been classified into three families: the HECT (homologous to E6-AP COOH terminus) family (Hershko and Ciechanover, 1998; Huibregtse et al., 1995), the RING-finger-containing protein family (Freemont, 2000; Joazeiro and Weissman, 2000; Lorick et al., 1999) and the U-box family (Aravind and Koonin, 2000; Cyr et al., 2002; Hatakeyama et al., 2001).

Tripartite motif (TRIM) proteins are characterized by the presence of a RING finger, one or two zinc-binding motifs called B-boxes, an associated coiled-coil region and C-terminal unique domains (Meroni and Diez-Roux, 2005; Nisole et al., 2005; Reymond et al., 2001). TRIM family proteins are involved in a broad range of biological processes and their alterations often cause diverse pathological conditions, such as developmental disorders, neurodegenerative diseases, viral infection and carcinogenesis (Kano et al., 2008; Miyajima et al., 2008; Quaderi et al., 1997).

TRIM containing 6 (TRIM6), a member of the TRIM family (Ozato et al., 2008), also has C-terminal PRY and SPRY (SPla kinase and RYanodine receptor) domains. The *TRIM6* gene is mapped to chromosome 11p15, where it locates within one of the *TRIM* gene clusters. It has also been reported that TRIM6 is localized to cytoplasmic bodies of variable size or nuclear sticks in U2OS and HeLa cells (Reymond et al., 2001). However, the molecular function of TRIM6 has not yet been elucidated.

The proto-oncogene product Myc, a basic helix-loop-helix–leucine zipper (bHLH/LZ)-type transcription factor, is a master regulator of cell proliferation. Myc is transiently expressed and its activity is directly related to the proliferative potential of cells. Wild-type Myc is usually unstable in proliferating cells, whereas mutant Myc, which is often expressed in B cell lymphoma cells, is stable. It has been reported that the ubiquitin–proteasome system controls the abundance of several proteins, especially short-lived regulatory proteins, including Myc. The expression level of the Myc protein must be carefully regulated to avoid carcinogenic transformation.

It has recently been reported that Myc has an important role in the proliferation and maintenance of the pluripotency of embryonic stem (ES) cells. Induced pluripotent stem cells (iPS cells) have been established by expressing four genes, *Oct3/4* [POU class 5 homeobox 1 (*Pou5f1*)], SRY (sex determining region Y)-box 2 (*Sox2*), Kruppel-like factor 4 (*Klf4*) and *Myc*, into fibroblasts of mice and humans (Takahashi and Yamanaka, 2006). However, the potential carcinogenicity of Myc must be suppressed to establish iPS cells for clinical application. Thus, efforts have been made to generate iPS cells without using *Myc* (Nakagawa et al., 2008; Okita et al., 2008). However, if *Myc* is not used, the efficiency of iPS cell establishment is very low. Therefore, appropriate regulation of the expression level of Myc

Journal of Cell Science

at a particular stage of stem cell development is thought to be important for maintaining the pluripotency of those cells (Takayama et al., 2010).

In this study, we performed yeast two-hybrid screening using TRIM6 as bait with the aim of elucidating the molecular function of TRIM6, which is selectively expressed in ES cells. We identified Myc as a TRIM6-interacting protein and found that TRIM6 negatively regulated the transcriptional activity of *Myc* and maintained the pluripotency of ES cells. These findings indicate that TRIM6 acts as a corepressor of Myc in mouse ES cells.

Results

TRIM6 interacts with Myc

To examine the molecular function of TRIM6, we isolated TRIM6-interacting proteins from a mouse T cell cDNA library by using a yeast two-hybrid system. We obtained seven positive clones from 3.5×10^5 transformants. One of the positive clones had sequence identities with cDNA encoding mouse Myc (Fig. 1A). To examine whether TRIM6 interacts with Myc in mammalian cells, we performed an in vivo binding assay using cells transfected with expression vectors. We expressed haemagglutinin (HA)-tagged full-length TRIM6 together with FLAG-tagged Myc in HEK293T cells. Cell lysates were subjected to immunoprecipitation with an anti-FLAG antibody, and the resulting precipitates were subjected to immunoblot analysis with an anti-HA antibody. FLAG-tagged Myc was co-precipitated with HA-tagged TRIM6, indicating that Myc specifically binds to TRIM6 in mammalian cells (Fig. 1B). Next, to examine whether the RING-finger domain is required for the interaction between TRIM6 and Myc, we generated a deletion mutant form of TRIM6 lacking the RING-finger domain [TRIM6(ΔR)] (Fig. 1C). An in vivo binding assay showed that TRIM6(ΔR) also interacted with Myc in HEK293T cells, indicating that the RING-finger domain is not required for the interaction between TRIM6 and Myc (Fig. 1D).

Phosphorylation of T58 and S62 of Myc does not affect the interaction of TRIM6 with Myc

It has been reported that phosphorylation of threonine-58 (T58) and serine-62 (S62) in Myc box 1 (MB1) is crucial for the stability of Myc and that these two residues are often mutated in various tumor types (Fig. 2A) (Bahram et al., 2000; Lutterbach and Hann, 1994). To determine whether phosphorylation of T58 and S62 in the MB1 of Myc is required for the binding of Myc to TRIM6, we performed an in vivo binding assay using TRIM6 and Myc mutants (T58A, S62A and T58A/S62A) in which either or both T58 and S62 were substituted for alanine to inhibit phosphorylation. We expressed HA-tagged TRIM6 together with FLAG-tagged Myc mutants in HEK293T cells. Cell lysates were subjected to precipitation with an anti-HA antibody and the resulting immunoprecipitates were subjected to immunoblot analysis with an anti-FLAG antibody. FLAG-tagged Myc wild-type and mutants were detected in anti-HA immunoprecipitates, suggesting that phosphorylation within the MB1 of Myc is not required for the interaction between TRIM6 and Myc (Fig. 2B). Next, to determine whether TRIM6 ubiquitinated Myc, we performed an in vivo ubiquitination assay. Expression vectors encoding FLAG-tagged Myc, HA-tagged TRIM6 and His_6-tagged-ubiquitin were transfected into HEK293T cells. Whole-cell lysates were subjected to pull-down with Ni-NTA agarose using denatured conditions with 8 M urea to inhibit noncovalent binding; the resulting precipitates were subjected to immunoblot analysis with anti-FLAG and anti-His_6 antibodies. Immunoblot analysis showed that overexpression of TRIM6 caused extensive ubiquitination of

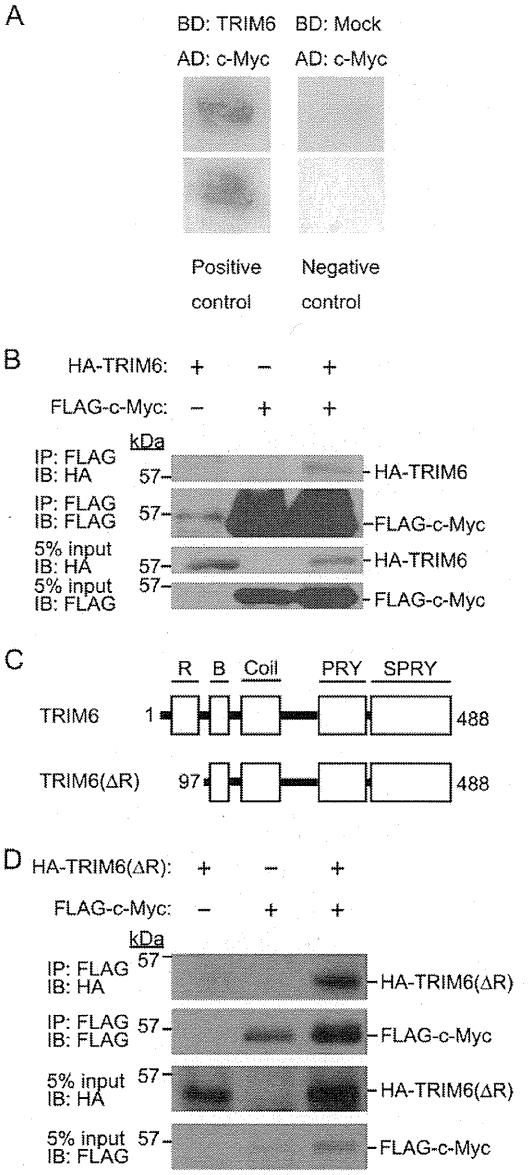

Fig. 1. TRIM6 interacts with Myc. (**A**) Yeast two-hybrid screening for TRIM6-interacting proteins using a mouse T cell cDNA library. pBMT116 and pACT2 vectors were used as negative controls. CHIP and EKN1 cDNAs were used for positive controls. (**B**) In vivo binding assay between TRIM6 and Myc. Expression vectors encoding FLAG-tagged Myc and HA-tagged TRIM6 were transfected into HEK293T cells. Cell lysates were immunoprecipitated with an anti-FLAG antibody and immunoblotted with anti-HA and anti-FLAG antibodies. (**C**) Schematic representation of TRIM6 and a deletion mutant. R, Ring-finger domain; B, B-box domain; Coil, coiled-coil domain; PRY, PRY domain; SPRY, SPRY domain. (**D**) Interaction between TRIM6(ΔR) and Myc in vivo. Expression vectors encoding FLAG-tagged Myc and HA-tagged TRIM6(ΔR) were transfected into HEK293T cells. Cell lysates were immunoprecipitated with anti-FLAG antibody and immunoblotted with anti-HA and anti-FLAG antibodies.

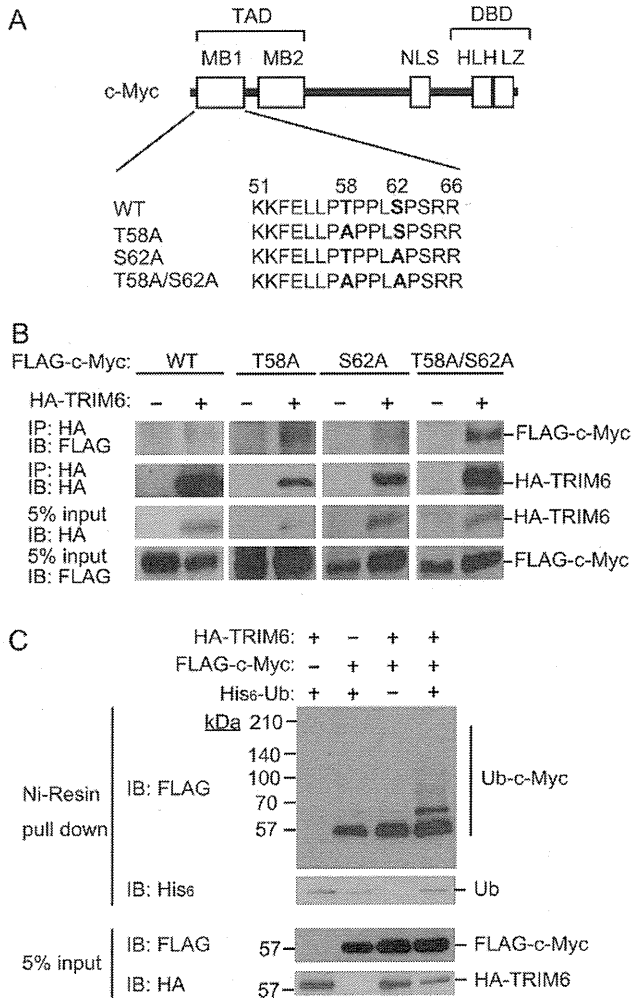

Fig. 2. TRIM6 binds to Myc in a phosphorylation-independent manner at T58 and S62 and mediates Myc ubiquitination. (**A**) Schematic representation of Myc mutants. There are two phosphorylation sites, T58 and S62, in the N-terminus of Myc. DBD, DNA-binding domain; NLS, nuclear localization signal; TAD, transactivation domain. Three Myc mutants in which T58 and/or S62 were substituted for alanine (A) are shown. (**B**) TRIM6 also interacted with Myc mutants that were not phosphorylated at T58 or S62. Expression vectors encoding HA-tagged TRIM6 and FLAG-tagged Myc mutants were transfected into HEK293T cells. Cell lysates were immunoprecipitated with anti-HA antibody and immunoblotted with anti-FLAG and anti-HA antibodies. (**C**) In vivo ubiquitination assay of Myc by TRIM6. Expression vectors encoding FLAG-tagged Myc, HA-tagged TRIM6 and His_6-tagged ubiquitin were transfected into HEK293T cells. Cell lysates were used for a pull-down assay with Nickel-affinity resin and immunoblotted with antibodies against FLAG-tag, His_6-tag or HA-tag.

Myc (Fig. 2C). These findings suggest that TRIM6 interacts with and ubiquitinates Myc without phosphorylation of T58 and S62 on Myc.

TRIM6 represses transcriptional activation of Myc

To determine whether TRIM6 affects Myc-mediated transcription, we performed a luciferase reporter assay using a p4 × E-SVP-Luc reporter plasmid in HEK293T cells (Fig. 3A). The luciferase assay showed that expression of FLAG-tagged Myc induced luciferase activity, whereas overexpression of TRIM6 repressed Myc-mediated transcriptional activity. The luciferase assay also showed that TRIM6 attenuated Myc transcriptional activity in a dose-dependent manner (Fig. 3A). Interestingly, the TRIM6(ΔR) mutant also repressed Myc transcriptional activity in a dose-dependent fashion, but its effect was slightly weaker than that of wild-type TRIM6, suggesting that the RING domain of TRIM6 is important to some degree for suppression of Myc-mediated transcription by TRIM6.

Next, by using a retroviral expression system, we generated Namalwa cells and NIH 3T3 cells in which FLAG-tagged TRIM6 was stably expressed (Fig. 3B). We examined the effect of TRIM6 on the abundance of endogenous Myc using Namalwa cells stably expressing TRIM6. However, the amount of Myc in these cells did not differ from the amount of Myc in Namalwa cells infected with the corresponding empty vector (Fig. 3C). Furthermore, the growth rate of Namalwa cells expressing TRIM6 was similar to that of cells infected with the corresponding empty vector (Fig. 3D). To determine whether TRIM6 affects the stability of Myc in vivo, we performed a protein stability analysis to verify the effect of TRIM6 on the stability of endogenous Myc in NIH 3T3 cells. The protein stability analysis showed that the stability of Myc in cells expressing TRIM6 was similar to that in mock transfectants (Fig. 3E,F). These findings suggest that TRIM6 suppresses Myc-mediated transcription but that its suppression does not affect cell proliferation and that TRIM6 does not change the stability of Myc.

TRIM6 is highly expressed in ES cells and interacts with endogenous Myc

To examine the expression profiles of TRIM6, we compared the protein levels of TRIM6 in various mouse cell lines from different tissues: ES cell line E14, primary embryonic fibroblasts (PEF), embryonic carcinoma cell line P19, myoblast cell line C2C12, fibroblast cell line NIH3T3 and neuroblastoma cell line neuro2a. Immunoblot analysis showed that TRIM6 was highly expressed in mouse embryonic stem cells but not in PEF (Fig. 4A). In addition, TRIM6 was slightly expressed in mouse P19 cells, which have the potential to transform into teratocarcinoma cells. We then verified the interaction between endogenous TRIM6 and Myc using E14 cells by immunoprecipitation with an anti-Myc antibody (Fig. 4B). Immunofluorescence analysis showed that FLAG-tagged TRIM6 was localized predominantly in the cytosol and weakly in the nucleus, whereas endogenous Myc was localized predominantly in the nucleus. Moreover, we found that TRIM6 partially overlapped with Myc in the intranuclear or perinuclear region (Fig. 4C).

TRIM6 represses Myc-mediated transcription in ES cells

To examine whether TRIM6 affects Myc-mediated transcription in not only HEK293T cells, but also ES cells, we performed a luciferase reporter assay using p4 × E-SVP-Luc in ES cells. First, we verified that endogenous Myc was expressed in the mouse ES cell lines E14 and TC-1 1 (Fig. 5A). We transiently transfected an expression vector encoding FLAG-tagged TRIM6 with the p4 × E-SVP-Luc reporter plasmid. Luciferase assays using ES cells showed that TRIM6 repressed endogenous Myc-mediated transcriptional activity as was observed in the luciferase assay

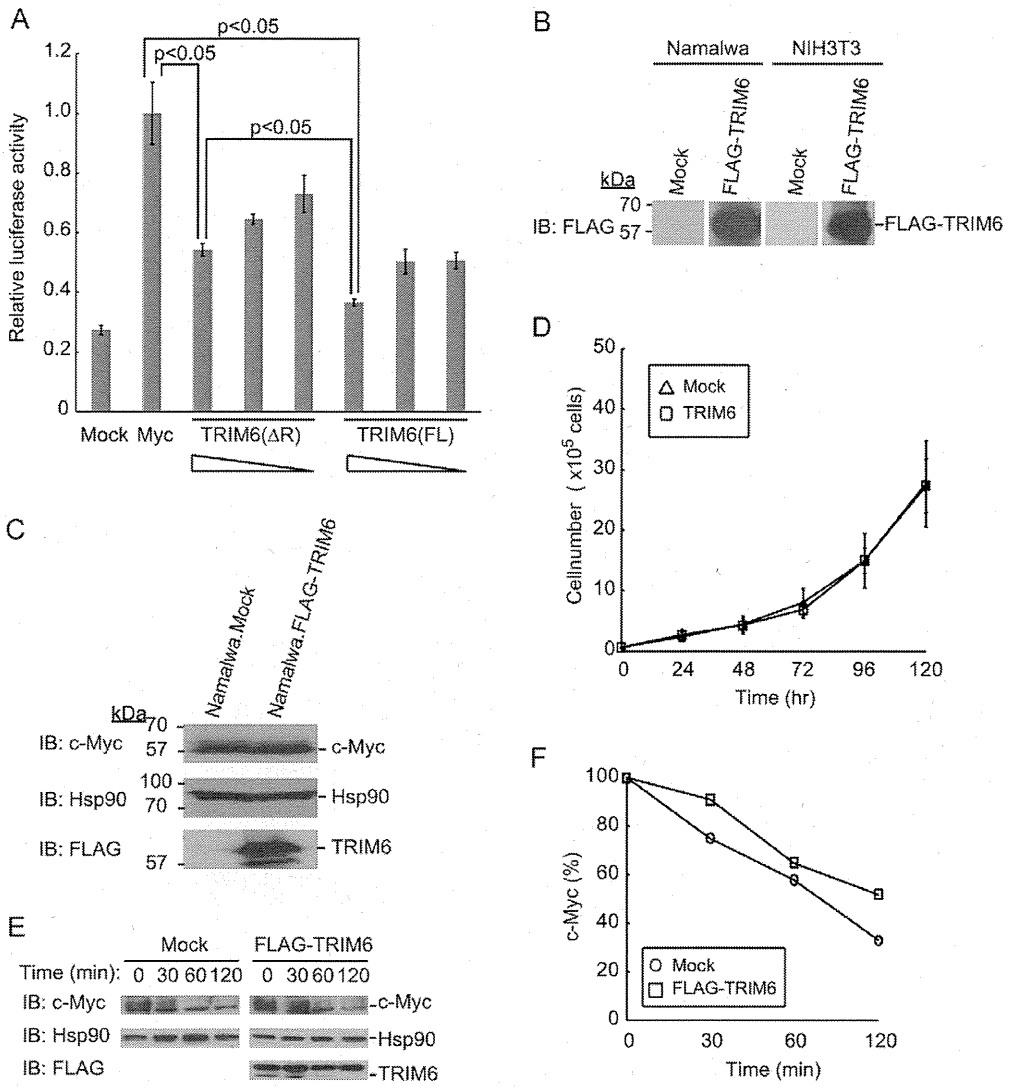

Fig. 3. TRIM6 represses Myc-mediated transcriptional activity. (**A**) TRIM6 represses Myc-mediated transcriptional activity in a dose-dependent manner. The p4 × E-SVP-Luc reporter vector and expression vector encoding various amounts of TRIM6 (FL) or TRIM6(ΔR) were transfected into HEK293T cells. Forty-eight hours after transfection, cells were harvested and assayed for luciferase activity. Data are mean ± standard deviation (SD) of values from three independent experiments. *P* values for indicated comparisons were determined by the Student's *t* test. (**B**) Establishment of Namalwa cell lines and NIH 3T3 cell line stably expressing FLAG-tagged TRIM6 by a retroviral expression system. The cell lines were checked by immunoblot analysis using anti-FLAG antibody. (**C**) TRIM6 does not affect the expression level of endogenous Myc in a Bürkitt lymphoma cell line. Namalwa cells infected with either a retroviral vector encoding FLAG-tagged TRIM6 or the corresponding empty vector (Mock) were lysed and subjected to immunoblot analysis with antibodies to Myc, Hsp90 and FLAG. Anti-Hsp90 antibody was used as an internal control. (**D**) TRIM6 does not affect cell proliferation. Namalwa cells transfected with FLAG-tagged TRIM6 and mock (2×10^4 cells) were seeded in 60-mm dishes and harvested for counting cell numbers at the indicated times. Data are mean ± SD of values from three independent experiments. (**E**) Protein stability analysis of endogenous Myc in cells stably expressing TRIM6. NIH3T3 cells stably expressing FLAG-tagged TRIM6 and Mock were used for a protein stability assay with cycloheximide. Twenty-four hours after seeding on dishes, the cells were cultured in the presence of cycloheximide (50 μg/ml) for the indicated times. Cell lysates were then subjected to immunoblot analysis with anti-Myc, anti-Hsp90 or anti-FLAG antibody. (**F**) Intensity of the endogenous Myc bands in the protein stability analysis in E was normalized with that of the corresponding Hsp90 bands and then expressed as a percentage of the normalized value for time zero.

using HEK293T cells (Fig. 5B). Furthermore, assays using E14 cells showed that TRIM6 attenuated endogenous Myc-mediated transcriptional activity in a dose-dependent manner (Fig. 5B). Next, by using electroporation, we generated three E14 cell lines in which FLAG-tagged TRIM6 was stably expressed (Fig. 5C), and we performed luciferase assays to compare the transcriptional activity of endogenous Myc by using these cell lines. Luciferase assays also showed that TRIM6 repressed endogenous Myc transcriptional activity in E14 cells (E14.TRIM6-1) (Fig. 5D). Moreover, we examined the effect of TRIM6 on the expression level of endogenous Myc. Overexpression of TRIM6 caused no significant change in the

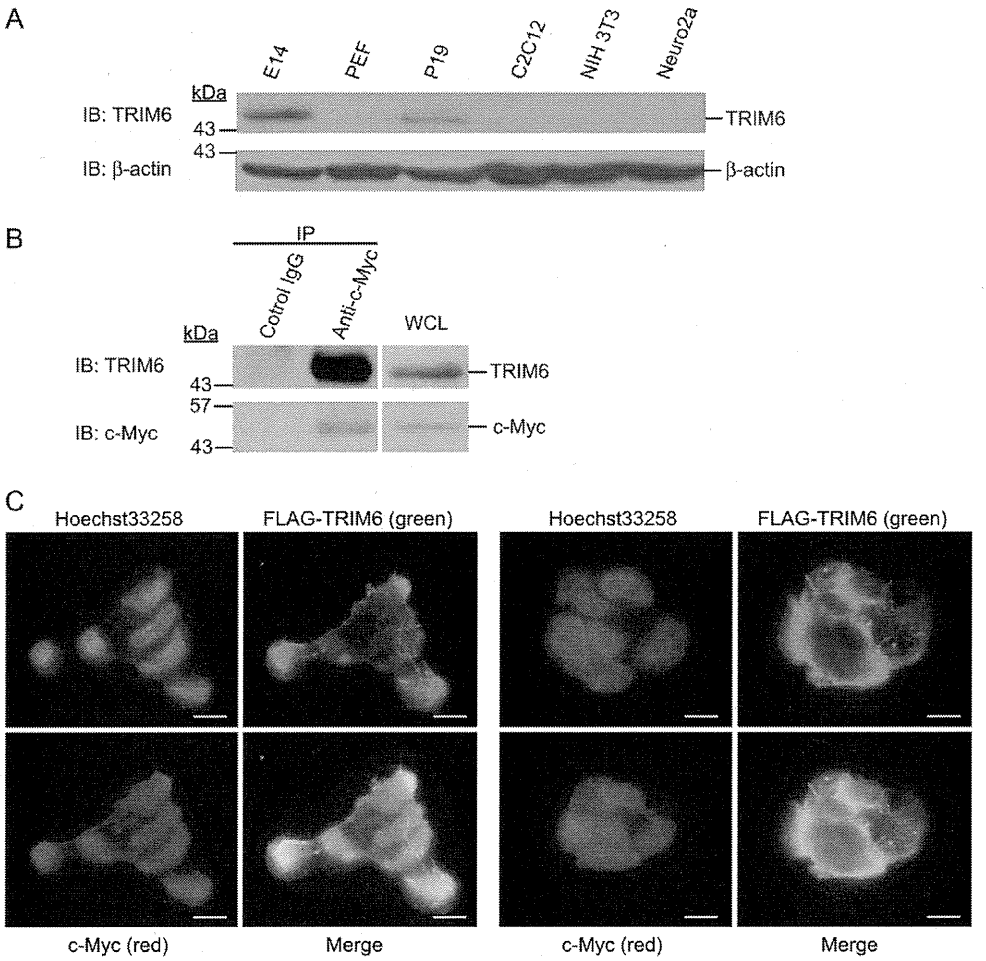

Fig. 4. TRIM6 is selectively expressed in ES cells and interacts with endogenous Myc in ES cells. (**A**) Expression of TRIM6 in various cell lines. Cell lysates from the indicated cell lines were subjected to immunoblot analysis with anti-TRIM6 and anti-β-actin antibodies. (**B**) Interaction between endogenous TRIM6 and Myc in ES cells. Cell lysates from E14 cells were immunoprecipitated with anti-Myc antibody or Mock [control immunoglobulin (IgG)] and immunoblotted with an antibody to TRIM6. (**C**) Colocalization of FLAG-tagged TRIM6 and endogenous Myc by immunofluorescence analysis. E14 cells stably expressing FLAG-tagged TRIM6 were used for the analysis. The cells were fixed and stained with antibodies to FLAG (green), Myc (red) or Hoechst 33258 (blue). Scale bars: 20 μm.

expression level of Myc in E14 cells (Fig. 5E). To verify that TRIM6 affects the stability of endogenous Myc in vivo, we performed a protein stability analysis using cycloheximide and these E14 cell lines. The analysis showed that the degradation rate of endogenous Myc was similar in E14 cells stably expressing TRIM6 to that in mock cells (Fig. 5F). However, overexpression of TRIM6 in E14 cells caused high expression of NANOG, which is an important pluripotent marker of ES cells, suggesting that TRIM6 regulates cell differentiation via Myc-mediated transcription (Fig. 5E). To determine whether forced expression of TRIM6 renders leukemia inhibitory factor (LIF) redundant in ES cells, as in the case of NANOG and KLF4 overexpression (Chan et al., 2009; Darr et al., 2006), we observed E14 cells stably expressing TRIM6 and mock cells without LIF. Although overexpression of TRIM6 in E14 cells caused high expression of NANOG, forced expression of TRIM6 could not maintain the undifferentiation of ES cells without LIF (Fig. 5G). Immunoblot analysis showed that the expression levels of NANOG were decreased in E14 cells stably expressing TRIM6 as well as in mock cells after culture without LIF (Fig. 5H). These findings suggest that forced expression of TRIM6 cannot maintain the pluripotency of ES cells without LIF.

High expression of Myc induced by TRIM6 knockdown in ES cells

To clarify why TRIM6 modulates Myc transcriptional activity in ES cells and does not affect the stability of endogenous Myc by ectopic overexpression of TRIM6, we next generated ES cell lines in which TRIM6 was knocked down. Short hairpin RNAs (shRNAs) targeting TRIM6 were introduced into E14 cells by using a retroviral infection system; silencing of TRIM6 at the protein level in E14 cells was confirmed by immunoblot analysis with an anti-TRIM6 antibody (Fig. 6A). Immunoblot analysis showed that the amount of endogenous Myc in E14 cells in which TRIM6 was knocked down was larger than in mock cells, whereas the expression level of NANOG in TRIM6-knockdown

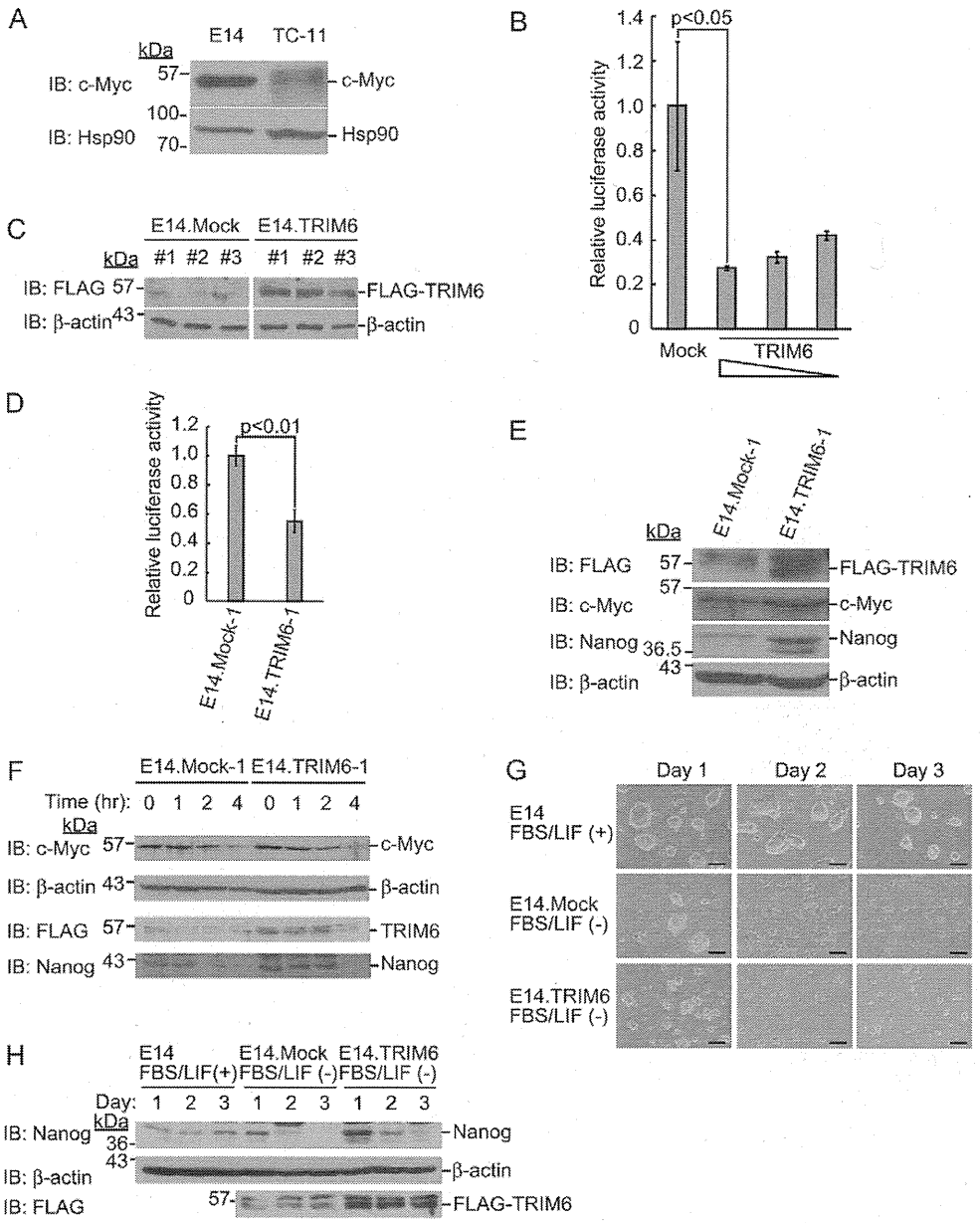

Fig. 5. TRIM6 inhibits transcriptional activation of Myc in ES cells. (**A**) Expression of Myc in mouse ES cell lines. Cell lysates from mouse ES cell lines E14 and TC-11 were subjected to immunoblot analysis with anti-Myc antibody. (**B**) TRIM6 represses Myc-mediated transcriptional activity in a dose-dependent manner. p4 × E-SVP luciferase reporter vector, pRL-TK *Renilla* vector and various amounts of TRIM6 expression vector were transiently transfected into E14 cells. Forty-eight hours after culture with LIF, the cells were harvested and assayed for luciferase activity. (**C**) Establishment of three E14 cell lines stably expressing FLAG-tagged TRIM6 by using electroporation followed by puromycin selection. These cell lines were checked by immunoblot analysis using anti-FLAG antibody. (**D**) TRIM6 represses Myc-mediated transcriptional activity in ES cells stably expressing TRIM6. E14 cell lines stably expressing TRIM6 were assayed for luciferase activity. (**E**) Effect of endogenous Myc and NANOG expression by overexpression of TRIM6 in ES cells. E14 cell lines stably expressing FLAG-tagged TRIM6 and Mock cells were lysed and subjected to immunoblot analysis with antibodies to FLAG, Myc, NANOG and β-actin. (**F**) Protein stability analysis of endogenous Myc in ES cells stably expressing TRIM6. An E14 cell line stably expressing FLAG-tagged TRIM6 and a Mock were used for a protein stability analysis with cycloheximide. The cells were incubated in a conditioned medium including LIF in the presence of cycloheximide (50 μg/ml) for the times indicated. Cell lysates were then subjected to immunoblot analysis with anti-Myc, anti-β-actin, anti-NANOG or anti-FLAG antibody. (**G**) Forced expression of TRIM6 cannot maintain the pluripotency of ES cells without LIF. E14 cell lines with stable overexpression of TRIM6 or Mock cells were seeded at 1×10^6 cells in 60-mm dishes coated with gelatin. These ES cells were cultured with a conditioned medium including 15% FBS. As control, E14 cells were also cultured with the same medium and LIF. Day 1 is the day that each cell line was seeded on dishes. The culture medium with or without LIF was changed daily. Scale bars: 100 μm. (**H**) Immunoblot analysis of NANOG in TRIM6-overexpressing ES cells without LIF. E14 cell lines with stable overexpression of TRIM6 or mock cells were seeded in 60-mm dishes coated with gelatin, and immunoblot analysis with anti-NANOG antibody was performed at the indicated times after seeding. As a control, E14 cells were also analyzed with the same medium and LIF. Two independent experiments were performed. Anti-β-actin antibody was used as an internal control.

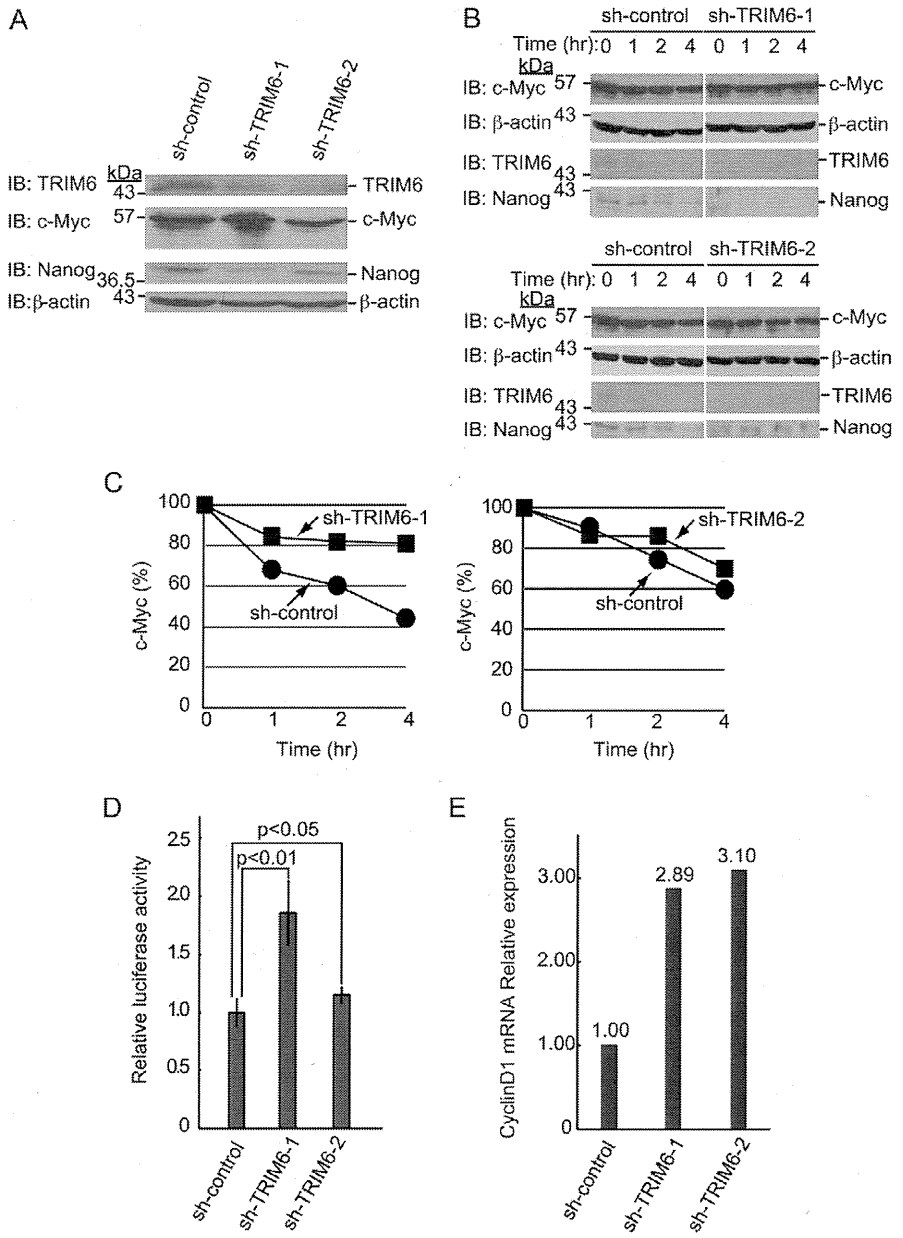

Fig. 6. Effect of silencing TRIM6 on the expression of endogenous Myc and NANOG in ES cells. (**A**) Knockdown of TRIM6 facilitates Myc expression in ES cells. shRNAs targeting TRIM6 (sh-TRIM6-1 and sh-TRIM6-2) or scrambled shRNA as a negative control (sh-control) were introduced into E14 cells using a retroviral expression system. Cells were lysed and subjected to immunoblotting with anti-TRIM6, anti-Myc, anti-Nanog and anti-β-actin antibodies. (**B**) Protein stability analysis of endogenous Myc in knockdown E14 cell lines with sh-TRIM6 or sh-control. E14 cell lines stably knocked-down with sh-TRIM6-1, sh-TRIM6-2 and sh-control were used for a protein stability analysis with cycloheximide. Cell lysates were then subjected to immunoblot analysis with anti-Myc, anti-β-actin, anti-Nanog or anti-FLAG antibody. (**C**) Intensity of the endogenous Myc bands in the protein stability analysis in B was normalized with that of the corresponding β-actin bands and was then expressed as a percentage of the normalized value for time zero. Data are means of values from two independent experiments. (**D**) Knockdown of TRIM6 facilitates Myc-mediated transcriptional activity in ES cells. p4 × E-SVP luciferase reporter vector and pRL-TK *Renilla* vector were transfected into knockdown E14 cell lines silenced with sh-TRIM6. Data are mean ± SD of values from three independent experiments. (**E**) Knockdown of TRIM6 causes upregulation of *Ccdn1* expression in ES cells. mRNAs of *Ccdn1* were measured by real-time quantitative PCR. The relative *Ccdn1* mRNA expression level in cells that had been transfected with sh-control was defined as 1.

E14 cells was less than that in control cells. To confirm that knockdown of TRIM6 affected the stability of endogenous Myc, we performed a protein stability analysis using these knockdown ES cells. The analysis showed that knockdown of TRIM6 caused high stability of Myc (Fig. 6B,C). To further examine the effect of TRIM6 on Myc-mediated transcription, we performed a relative luciferase assay using these knockdown ES cells. The assay showed that Myc-mediated transcriptional activities were increased in TRIM6-knockdown cells compared with those in cells treated with control shRNA (Fig. 6D). In addition, real-time PCR using these cell lines was performed to analyze the mRNA level of the gene encoding cyclin D1 (*Ccdn1*), given that *Ccdn1* is one of the target genes of Myc (Daksis et al., 1994; Dang, 1999; Perez-Roger et al., 1999). Consistent with the results of Myc-dependent transcriptional activity shown by the luciferase assay, the mRNA level of *Ccdn1* was positively regulated in TRIM6-knockdown cells compared with that in control cells (Fig. 6E). These findings suggest that TRIM6 regulates Myc-mediated transcriptional activity and affects the expression levels of target genes of Myc in ES cells.

Knockdown of TRIM6 promotes differentiation of ES cells

Given that our results showed that TRIM6 modulated the expression level of Myc in ES cells and that knockdown of TRIM6 in ES cells caused a decrease in the expression level of NANOG, we hypothesized that the expression of TRIM6 is also changed in several differentiation stages of ES cells. We first performed real-time PCR to quantify the mRNA level of *TRIM6*

in differentiated and undifferentiated ES cells. As expected, the relative mRNA level of *TRIM6* was significantly decreased in differentiated ES cells cultured without LIF compared with the level in undifferentiated ES cells (Fig. 7A,B). We also compared the level of TRIM6 protein in differentiated and undifferentiated ES cells. The expression level of TRIM6 was higher in undifferentiated than in differentiated ES cells (Fig. 7C). Despite the high expression level of TRIM6, the Myc protein expression level was significantly higher in undifferentiated than in differentiated ES cells (Fig. 7C).

Next, to examine whether TRIM6 maintains the undifferentiated state of ES cells, we evaluated the morphological phenotype of ES cells with or without endogenous TRIM6 expression. We seeded each cell line on dishes and cultured the cells with LIF for maintenance of pluripotency. Colonies from control E14 cells grew normally and were enlarged in the presence of LIF for 3 days, whereas TRIM6-knockdown E14 cells (sh-TRIM6-1) differentiated into endoderm-like cells even in the presence of LIF (Fig. 7D). Moreover, we checked the expression levels of NANOG, GATA-binding protein 4 (GATA-4) and alpha-fetoprotein (AFP), which are endodermal differentiation markers in ES cells, and the expression levels of heart and neural crest derivatives expressed 1 (HAND1) and microtubule-associated-protein-2 (MAP2), which are ectodermal differentiation markers in ES cells, by immunoblot analysis at the indicated times (Knofler et al., 2002; Kwon et al., 2006; Soudais et al., 1995; Tropepe et al., 2001). Immunoblot analysis showed that the expression level of NANOG in TRIM6-knockdown E14 cells (sh-TRIM6-1) was lower than in mock cells, whereas the expression levels of GATA-4 and AFP in TRIM6-knockdown E14 cells were higher than in mock cells (Fig. 7E). By contrast, little, if any, HAND1 and MAP2 protein could be detected in either cell line (Fig. 7E). These findings indicated that silencing of TRIM6 in ES cells induced a decrease in NANOG expression level and tended to induce differentiation to endodermal cells rather than ectodermal cells, suggesting that TRIM6 is required for the maintenance of an undifferentiated state of ES cells in the presence of LIF.

To determine whether differentiation induced by TRIM6 knockdown is rescued by transduction of exogenous NANOG, we tried to generate stably NANOG-expressing E14 cell lines in which TRIM6 was knocked down (Fig. 7F). Immunoblot analysis showed that E14 cells in which TRIM6 was knocked down expressed NANOG and OCT3/4, which is encoding by another self-renewal and undifferentiation marker gene in ES cells, at lower levels than in mock cells. However, immunoblot analysis showed that the amount of OCT3/4 was recovered by overexpression of exogenous NANOG, suggesting that differentiation of TRIM6-knockdown cells is rescued by induction of exogenous NANOG and that TRIM6 mainly participates in regulation to maintain the pluripotency of ES cells at a site upstream of NANOG (Fig. 7F).

Furthermore, we checked the morphological phenotype of ES cell lines in which TRIM6 was knocked down and performed immunoblot analysis to confirm the expression levels of NANOG and OCT3/4 in ground-state culture (Ying et al., 2008). For the ground-state culture, pre-formulated NDiff N2B27 base medium was prepared with CHIR99021, which is a specific glycogen synthase kinase 3β (GSK3β) inhibitor, and PD0325901, which is a mitogen-activated protein kinase (MAPK) inhibitor, as two inhibitors (2i). E14 cells as control cells (E14 N2B27+2i), E14 cell lines in which TRIM6 was knocked down (sh-TRIM6 N2B27+2i) and sh-control cells (sh-control N2B27+2i) showed undifferentiated colony formation in the ground-state culture (Fig. 7G). Immunoblot analysis showed that the expression levels of NANOG and OCT3/4 protein were maintained in TRIM6-knockdown E14 cells (sh-TRIM6) as well as in E14 cells and sh-control E14 cells after several passages by means of the ground-state culture (Fig. 7H). The Myc protein levels were downregulated by suppressing the extracellular signal-regulated kinase (ERK) signal in this condition, as previously reported (Fig. 7H) (Ying et al., 2008). These findings suggest that ES cell lines in which TRIM6 has been knocked down differentiate under stimulation of Ras–MAPK kinase (MEK)–ERK signaling cascades.

Discussion

In this study, we identified Myc as a TRIM6-interacting protein in ES cells and revealed molecular functions of TRIM6 in the pluripotency of ES cells. SKP1–CUL1–F-box protein complex (SCF)-type E3 ligases, including SCF^{skp2} and SCF^{Fbw7}, also interact with Myc. Skp2 interacts with Myc via Myc-box 2 (MB2) and the HLH-Zip domain and promotes its ubiquitination and transcriptional activation (Kim et al., 2003; von der Lehr et al., 2003); Fbw7 ubiquitinates and degrades Myc by recognizing phosphorylation on T58 and S62 in MB1 of Myc (Yada et al., 2004). Using yeast two-hybrid screening and immunoprecipitation, we showed that TRIM6 binds to Myc and, in addition, interacts with Myc regardless of its phosphorylation at T58 and S62. We also showed that TRIM6 lacking a RING domain interacts with Myc. These findings suggest that a RING domain of TRIM6 and MB1 domain of Myc are not required for the interaction between them.

Given that it has been reported that Myc is involved in regulation of cell proliferation and cell differentiation (van Riggelen et al., 2010), we further examined the relationship between TRIM6 and Myc-mediated transcription. By using a luciferase reporter assay, we found that TRIM6 functions as a negative regulator of Myc and that TRIM6 suppressed the transcriptional activity of Myc in HEK293T cells; however, ectopic expression of FLAG-tagged TRIM6 did not change the expression level of Myc and cell proliferation rates in Namalwa cells. Furthermore, ectopically expressed TRIM6 did not cause a change in Myc in NIH3T3 cells. Similar results were obtained in experiments using ES cells. These findings suggest that ectopically expressed TRIM6 suppresses transcriptional activity of Myc but does not have sufficient activity to alter the function of Myc to affect cell proliferation and cell differentiation. Recently, it was reported that Myc has important roles in self-renewal and cell fate determination in ES cells and often causes tumor formation when its activity is dysregulated (Cartwright et al., 2005). Furthermore, there is accumulating evidence that the activity level of Myc is high in undifferentiated ES cells. It has been reported that ectopic Myc expression maintains the pluripotency of mouse ES cells without LIF (Cartwright et al., 2005). However, it has also been reported that Myc promotes progenitor cell differentiation in some contexts (Watt et al., 2008; Wilson et al., 2004). It has been shown that OCT3/4, which has been reported to prevent differentiation directly, is appropriately regulated in undifferentiated mouse ES cells, suggesting that its deregulated expression induces differentiation of mouse ES cells (Niwa et al., 2000). Although the detailed molecular mechanisms are unclear, the expression levels of Myc might also be

appropriately regulated in mouse undifferentiated ES cells. Based on these results, we speculated that TRIM6 strictly modulates the expression level or activity of Myc to prevent differentiation of mouse ES cells. We found increased polyubiquitination of Myc by TRIM6 in the in vivo ubiquitination assay, suggesting that TRIM6 functions as a ubiquitin ligase for Myc in ES cells. However, the reason why the expression level of Myc is maintained in ES cells despite the fact that Myc-mediated transcriptional activation is repressed by TRIM6 remains to be determined. It was recently reported that mouse ES cell culture conditions using MAPK and GSK3β inhibitors render Myc dispensable and that ES cells are not necessarily dependent on Myc to maintain their specific features (Hishida et al., 2011). The same authors also reported that stabilized Myc suppresses MAPK signaling to maintain the pluripotency of ES cells, suggesting that Myc finely modulates the balance of LIF–signal transducer and

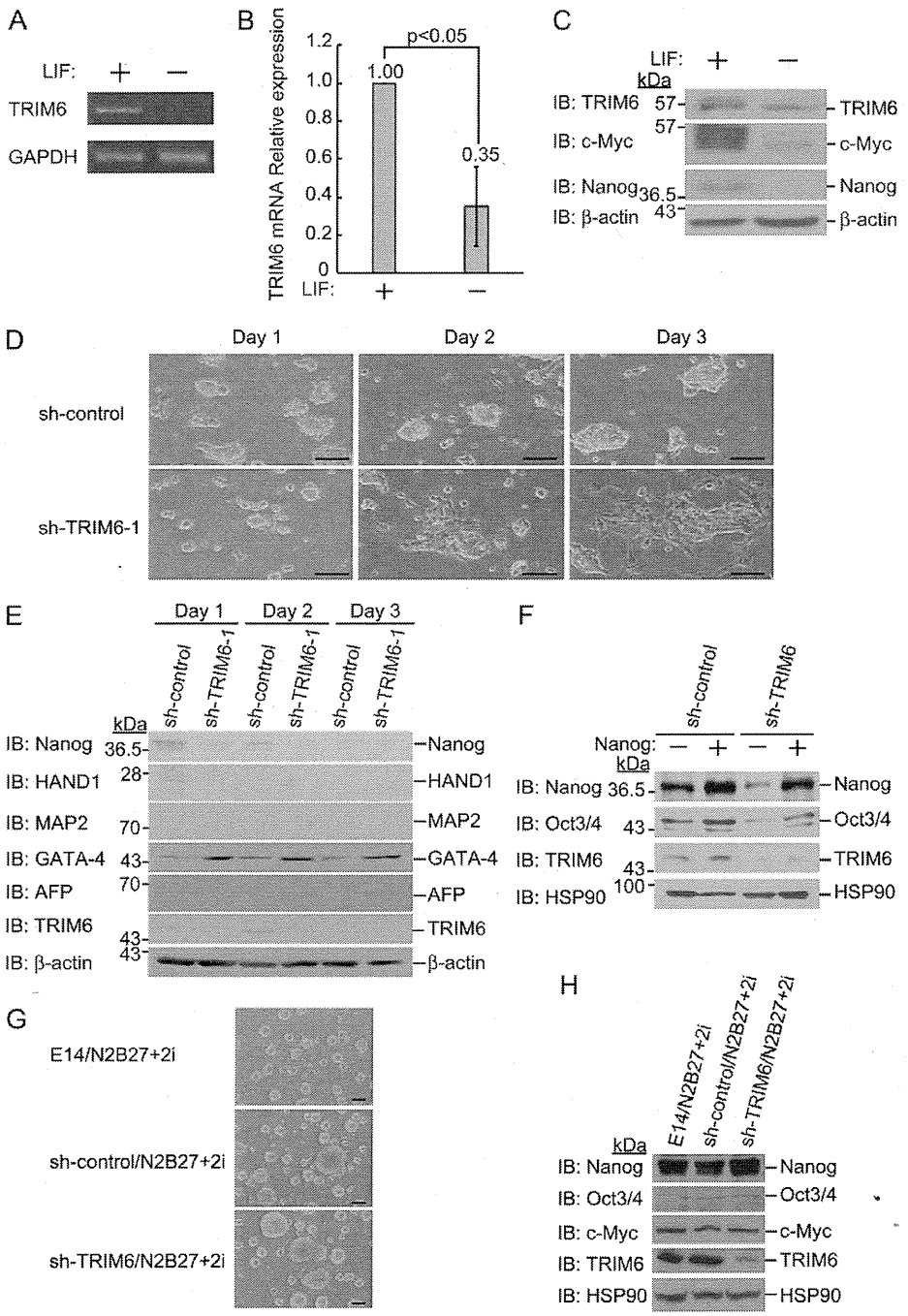

Fig. 7. See next page for legend.

activator of transcription 3 (STAT3) signaling and MAPK signaling activated by LIF and/or fibroblast growth factor (FGF), to prevent differentiation of ES cells. Based on our findings and the results of previous studies, we propose that TRIM6 is one of the interacting proteins that enable Myc to modulate its transcriptional activity appropriately. However, future work is needed to clarify the currently unknown mechanism that induces Myc expression in ES cells.

It has been reported that the pluripotency of ES cells is regulated by three intracellular transduction systems: the Janus kinase (JAK)-STAT3 pathway, phosphatidylinositol 3-kinase (PI3K)–AKT pathway and SHP2 [protein tyrosine phosphatase, non-receptor type 11 (PTPN11)]–RAS–MAPK pathway (Niwa et al., 1998; Watanabe et al., 2006). It has also been demonstrated that JAK–STAT3 and PI3K–AKT pathways are essential and sufficient to mediate LIF signals to maintain the pluripotency of ES cells (Niwa et al., 1998; Watanabe et al., 2006). By contrast, it has been shown that the SHP2–RAS–MAPK pathway, which is related to adjustment of the expression level of Myc, functions as a negative regulator of the maintenance of the pluripotency of ES cells (Kunath et al., 2007) and as a negative regulator of *Nanog* and the gene encoding T-box 3 (*Tbx3*) (Niwa et al., 2009). In our study, TRIM6 expression level was found to be higher in undifferentiated than in differentiated ES cells, and Myc expression level was found to be elevated in TRIM6-knockdown cells. These cells differentiated rapidly even in the presence of LIF. Therefore, TRIM6 could regulate Myc expression level within optimal ranges by repressing the transcription activity of Myc to maintain the pluripotency of undifferentiated ES cells. TRIM6 might also bind to Myc as a negative regulator of Myc in an undifferentiated state with LIF signaling. Upon differentiation of ES cells, TRIM6 is rapidly downregulated and Myc can be transiently activated. However, Myc protein might be degraded by another ubiquitin ligase or another proteolysis system independent of TRIM6 in the differentiated state, although the molecular mechanisms involved have not yet been clarified. Indeed, Myc has been shown to have roles in blocking cell differentiation and in maintaining progenitor cells in vivo (Knoepfler et al., 2002; Satoh et al., 2004). Therefore, TRIM6 probably functions as an important regulator of Myc expression and its downstream molecules to maintain the pluripotency of ES cells.

Recently, it has been reported that tripartite motif family-like 1 (TRIML1), one of the TRIM family proteins, is expressed in the embryo before implantation and that its knockdown causes a reduction in the number of blastocysts and failure to give rise to neonates after embryo transfer (Tian et al., 2009). Given that both TRIML1 and TRIM6 regulate the pluripotency and proliferation of ES cells and blastocysts, it will be important to analyze the functional interaction of TRIML1 and TRIM6 in future studies.

In conclusion, our study clarified that TRIM6 is highly expressed in ES cells and interacts with Myc to inhibit its transcriptional activity, followed by maintenance of pluripotency. Results of future studies aimed at clarifying the relationship between TRIM6 and interacting proteins, including Myc, should help advance understanding of developmental biology and cancer biology. Functional analysis of TRIM6 might provide benefits not only for the establishment of iPS cells, but also for their suppression in lymphomas and leukemias.

Fig. 7. TRIM6 is downregulated in differentiated ES cells and knockdown of TRIM6 induces ES cell differentiation. (**A**) *Trim6* mRNA expression is decreased in differentiated ES cells. The levels of *Trim6* mRNA derived from undifferentiated and differentiated ES cells were measured by real-time quantitative PCR. Differentiated E14 cells were cultured without LIF for 1 week. Amplified *Trim6* and *Gapdh* cDNAs were subjected to agarose gel electrophoresis. (**B**) Quantification of the amount of *Trim6* by real-time quantitative PCR using undifferentiated and differentiated ES cells in A. Data are means ± SD of values from three independent experiments. *P* values for indicated comparisons were determined by the Student's *t* test. (**C**) Immunoblot analysis of TRIM6 in undifferentiated and differentiated ES cells. Immunoblot analysis was performed with anti-TRIM6, anti-Myc, anti-Nanog and anti-β-actin antibodies. (**D**) Knockdown of TRIM6 induces ES cells differentiation. Stably knocked-down E14 cell lines with sh-TRIM6-1 or sh-control were seeded at 1×10^6 cells in 60-mm dishes coated with gelatin. These ES cells were cultured with a conditioned medium including 15% FBS and LIF. Day 0 is the day that each cell line was seeded on dishes. The culture medium with LIF was changed daily. Scale bars: 100 μm. (**E**) Immunoblot analysis of NANOG, HAND1, MAP2, GATA-4 and AFP in TRIM6-knockdown ES cells. Stably knocked-down E14 cell lines with sh-TRIM6-1 or sh-control were seeded at 1×10^6 cells in 60-mm dishes coated with gelatin, and immunoblot analysis with each antibody was performed at the indicated times after seeding. Two independent experiments were performed. Anti-β-actin antibody was used as an internal control. (**F**) Differentiation of TRIM6-knockdown cells is rescued by transduction of exogenous Nanog. By using a retroviral expression system, sh-TRIM6 or sh-control was introduced into E14 cells in which NANOG was stably expressed. Cells were lysed and subjected to immunoblotting with anti-OCT3/4, anti-NANOG, anti-TRIM6, and anti-HSP90 antibodies. Anti-HSP90 antibody was used as an internal control. (**G**) TRIM6-knockdown cells maintain an undifferentiated state in ground culture. Each ES cell line cultured for four passages (total of 14 days) in N2B27 base medium with CHIR99021 and PD0325901 (N2B27+2i) without serum and LIF. Scale bars: 100 μm. (**H**) Immunoblot analysis of NANOG and OCT3/4 in ES cells after 14 days in N2B27+2i culture. Myc protein expression level is suppressed in this condition. Anti-HSP90 antibody was used as an internal control.

Materials and Methods

Cell culture

HEK293T cells and NIH3T3 cells (ATCC, Manassas, VA) were cultured under an atmosphere of 5% CO_2 at 37℃ in DMEM (Sigma-Aldrich, St Louis, MO) supplemented with 10% fetal bovine serum (Invitrogen, Carlsbad, CA) or 10% calf serum (Camblex, Charles City, IA). Namalwa cells (ATCC) were cultured in RPMI-1640 (Sigma-Aldrich) with 10% fetal bovine serum (Invitrogen). Mouse ES E14 cells and TC-11 cells were cultured with or without feeder cells in DMEM (Invitrogen) supplemented with 15% heat-inactivated fetal bovine serum (Invitrogen), 55 μM β-mercaptoethanol (Invitrogen), 2 mM L-glutamine, 0.1 mM MEM non-essential amino acid and 1000 U/ml LIF (Millipore Corporation, Bedford, MA).

Yeast two-hybrid screening

Yeast strain L40 (*MAT***a** *LYS2::lexA-HIS3 URA3::lexA-lacZ trp1 leu2 his3*) (Invitrogen) was transformed both with the plasmid pBTM116 encoding the FLAG-tagged mouse TRIM6 and with a mouse T cell cDNA library in the pACT2 vector (Clontech, Mountain View, CA). The cells were then streaked on plates of medium lacking histidine to detect interaction-dependent activation of *HIS3* according to the manufacturer's protocol (Clontech).

Cloning of cDNA and plasmid construction

Mouse *Trim6* cDNA and mouse *Nanog* cDNA were amplified from ES cells by PCR with BlendTaq (Takara, Tokyo, Japan) using the following primers: 5′-ACAATGACTTCAACAGTCTTGGTG-3′ (*Trim6*-sense), 5′-ACCTCAGGAAG-TTGGCCGCCGCAG-3′ (*Trim6*-antisense), 5′-GACATGAGTGTGGGTCCTC-CT-3′ (*Nanog*-sense), and 5′-GTCTCATATTTCACCTGGTGG-3′ (*Nanog*-antisense). The amplified fragments were subcloned into pBluescript II SK^+ (Stratagene, La Jolla, CA), and the sequence was verified. Deletion mutants of *Trim6* cDNA containing amino acids 97–488, which was used as TRIM6 lacking a RING finger domain [TRIM6(ΔR)], were amplified by PCR and subcloned. A deletion mutant of the RING domain of TRIM6 was generated using the following primers: 5′-CGGACCTCCTATCAGCTGGG-3′ [TRIM6(ΔR)-sense] and 5′-AC-CTCAGGAAGTTGGCCGCCGCAG-3′ [TRIM6(ΔR)-antisense]. FLAG-tagged or HA-tagged TRIM6 and TRIM6(ΔR) cDNAs were then subcloned into the

vectors pCR (Invitrogen), pCGN and pCAG-puro for expression in eukaryotic cells. FLAG-tagged *Trim6* cDNAs were also subcloned into pBGK1 for expression in yeast. FLAG-tagged *Myc* cDNA and cDNAs of the FLAG-tagged Myc mutants T58A, S62A and T58A/S62A, which were subcloned into the pCI vector for expression in eukaryotic cells, have been described previously (Yada et al., 2004), as has His_6-tagged ubiquitin (Okumura et al., 2004). p4 × E-SVP-Luc was kindly provided by Hiroyoshi Ariga (Hokkaido University).

Recombinant proteins and antibodies

GST-fused TRIM6 was expressed in XL-1 Blue cells and then purified using glutathione-sepharose beads (GE Healthcare Bioscience, Piscataway, NJ). The recombinant TRIM6 protein was used as an immunogen in rabbits. A rabbit polyclonal anti-TRIM6 antibody was affinity purified using a recombinant TRIM6-conjugated sepharose 4B column. Other antibodies used in this study were as follows: anti-FLAG (1 μg/ml; M2 or M5, Sigma), anti-HA (1 μg/ml; HA.11, Covance Research Products, Berkeley, CA), anti-HA (1 μg/ml; Y11, Santa Cruz Biotechnology, Santa Cruz, CA), anti-His_6 (0.2 μg/ml; H-15, Santa Cruz Biotechnology), anti-Hsp90 (1 μg/ml; 68, BD, Franklin Lakes, NJ), anti-β-actin (0.2 μg/ml; AC15, Sigma), anti-Myc (1 μg/ml; N262, Santa Cruz Biotechnology and 1 μg/ml; 9E10, Covance Research Products), anti-GATA-4 (1 μg/ml; 6H10, Novus Biologicals, Littleton, CO), anti-HAND1 (1 mg/ml; GeneTex, Taiwan), anti-AFP (1:1000 dilution, 3H8, Cell Signaling Technology, Danvers, MA), anti-MAP2 (1:1000 dilution, #4542, Cell Signaling Technology), anti-Pou5f1 (Oct3/4) (1 μg/ml; mouse monoclonal, Abnova, Taiwan), and anti-Nanog (0.1 μg/ml; Abcam, Cambridge, MA).

Transfection, immunoprecipitation, and immunoblot analysis

HEK293T cells were transfected by the calcium phosphate method and lysed in a solution containing 50 mM Tris-HCl (pH 7.4), 150 mM NaCl, 1% Nonidet P-40, leupeptin (10 μg/ml), 1 mM phenylmethylsulfonyl fluoride, 400 μM Na_3VO_4, 400 μM EDTA, 10 mM NaF and 10 mM sodium pyrophosphate. The cell lysates were centrifuged at 16,000 ***g*** for 15 minutes at 4℃, and the resulting supernatant was incubated with antibodies for 2 hours at 4℃. Protein A-sepharose (GE Healthcare) that had been equilibrated with the same solution was added to the mixture, which was then tumbled for 1 hour at 4℃. The resin was separated by centrifugation, washed five times with ice-cold lysis buffer and then boiled in SDS sample buffer. Immune complexes were detected with primary antibodies, horseradish peroxidase-conjugated antibodies to mouse or rabbit IgG (1:10,000 dilutions, Promega) and an enhanced chemiluminescence system (GE Healthcare). For small-scale transfection, Fugene HD reagent (Roche, Mannheim, Germany) was used according to the manufacturer's protocol.

Ni-NTA pull-down assay

Cell lysates containing 8 M urea were used for purification of His_6-ubiquitin-conjugated proteins by chromatography on ProBond resin (Invitrogen) and proteins were then eluted from the resin with a solution containing 50 mM sodium phosphate buffer (pH 8.0), 100 mM KCl, 20% glycerol, 0.2% NP-40 and 200 mM imidazole (Okumura et al., 2004).

Establishment of stable transfectants by using a retrovirus expression system

Complementary DNAs were subcloned into pMX-puro or pMX-neo (kindly provided by Toshio Kitamura, Tokyo University). The resulting vectors were used to transfect Plat A or Plat E cells, and recombinant retroviruses were then generated (Morita et al., 2000). Forty-eight hours after transfection, culture supernatants were harvested and used for infection. The infection was carried out in the presence of polybrene at 8 μg/ml (Sigma-Aldrich). The infected clones were expanded and selected in a medium containing puromycin (1 μg/ml for E14 and NIH 3T3 and 5 μg/ml for Namalwa, Sigma-Aldrich) and G418 (250 μg/ml for E14, Sigma-Aldrich).

Establishment of stable transfectants of ES cells by using electroporation

E14 cells (2.5×10^7 cells) were electroporated with linearized pCAG-puro-FLAG-TRIM6 plasmid (20 μg) at 300 V and 125 μF twice by using Gene Pulser X cell (Bio-Rad Laboratories, Hercules, CA). The cells were plated onto 60-mm dishes and puromycin selection (1 μg/ml; Sigma-Aldrich) was initiated from 2 days after electroporation. After selection on a medium containing puromycin, the resulting cell lines were checked by immunoblot analysis with an anti-FLAG antibody.

RNA interference

pSUPER-retro-puro vector was purchased from OligoEngine. An shRNA for mouse TRIM6 mRNA was designed according to a previous report (Elbashir et al., 2002) and chemically synthesized (Invitrogen). pSUPER-retro-puro containing an shRNA for the mouse TRIM6 sequence (sh-TRIM6-1, 5′-GAGGCTCAG-AGAGGTTGCG-3′ or sh-TRIM6-2, 5′-GGGGCTGAGCATCATAGAA-3′) was constructed according to the manufacturer's protocol. We also used a scrambled shRNA as a negative control with no significant homology to any known gene sequences in the human or mouse genomes. Approximately 50% confluent HEK293 cells in 100-mm dishes were transfected with 10 μg pSUPER-retro-puro-shTRIM6 or scrambled shRNA vector together with 10 μg amphotrophic-packaging plasmid pCL10A1 using Fugene HD reagent (Roche). Forty-eight hours after transfection, culture supernatant containing retrovirus was collected, and retroviral supernatant was added to ES cells in 60-mm dishes with polybrene (8 μg/ml, Sigma-Aldrich). Cells were cultured with puromycin (1 μg/ml) and LIF for 1 week.

Dual-luciferase assay

Cells were seeded in 24-well plates at 1×10^5 cells or 5×10^4 cells per well for HEK293T or E14, respectively, and incubated at 37℃ with 5% CO_2 for 48 hours. A p4 × E-SVP-Luc reporter plasmid, pRL-TK *Renilla* luciferase plasmid (Promega) and various combinations of HA-tagged TRIM6 and/or FLAG-tagged Myc expression plasmid were transfected into cells using Fugene HD reagent (Roche). Forty-eight hours after transfection, the cell lysates were assayed for luciferase activity with a Dual-Luciferase Reporter Assay System (Promega) and quantified with a luminometer (Promega).

Protein stability assay with cycloheximide

Cells were cultured with cycloheximide (Sigma-Aldrich) at a concentration of 50 μg/ml and then incubated for the indicated times in each experiment.

Immunofluorescence staining

E14 cells expressing FLAG-tagged TRIM6 grown on a glass cover were fixed for 10 minutes at room temperature with 2% formaldehyde in PBS and then incubated for 1 hour at room temperature with a primary antibody to FLAG or Myc in PBS containing 0.1% bovine serum albumin and 0.1% saponin. The cells were then incubated with Alexa-Fluor-488-labeled goat polyclonal antibody to mouse IgG or Alexa-Fluor-546-labeled goat polyclonal antibody to rabbit IgG (Invitrogen) at a dilution of 1:1000. The cells were further incubated with Hoechst 33258 (1 μg/ml) in PBS for 10 minutes, followed by extensive washing with PBS, and then photographed with a CCD camera (DP71, Olympus) attached to an Olympus BX51 microscope.

Real-time PCR

Total RNA was isolated from E14 cells using ISOGEN (Nippon Gene, Tokyo, Japan), followed by reverse transcription (RT) by ReverTra Ace (Toyobo, Osaka, Japan). The resulting cDNA was subjected to real-time PCR with a StepOne machine and Power SYBR Green PCR master mix (Applied Biosystems, Foster City, CA). The average threshold cycle (Ct) was determined from independent experiments and the level of gene expression relative to *GAPDH* was determined. The primer sequences for *Trim6*, *Ccnd1* and *Gapdh* were as follows: *Trim6*, 5′-CGATCTCAGGAGCACCGTGGT-3′ and 5′-AGGATGCTTCGGAGCTGCTTA-3′; *Ccnd1*, 5′-CCTCTCCTGCTACCGCACAAC-3′ and 5′-GCGCAGGCTTG-ACTCCAGAAG-3′; and *Gapdh*, 5′-GCAAATTCCATGGCACCGT-3′ and 5′-TCGCCCCACTTGATTTTGG-3′.

ES cells in ground state culture

As previously described (Ying et al., 2008), pre-formulated NDiff N2B27 base medium (StemCells, Inc., Newark, CA) was prepared with CHIR99021 (Axon Medchem BV, Groningen, Netherlands) and PD0325901 (Sigma-Aldrich). Inhibitors were used at the following concentrations: CHIR99021, 3 μM; and PD0325901, 1 μM (2i). ES cells were routinely propagated by trypsinization and replating every 3 days, with a ratio of 1:10.

Statistical analysis

Student's *t*-test was used to determine the statistical significance of experimental data.

Acknowledgements

We would like to thank Toshio Kitamura (Tokyo University) and Hiroyoshi Ariga (Hokkaido University) for the plasmids and Yuri Soida for help in preparing the manuscript.

Funding

The work was supported, in part, by Grants-in-Aid for Scientific Research from the Ministry of Education, Culture, Sports, Science and Technology (18076001 and 21390087), Grant for Basic Science Research Projects from The Sumitomo Foundation, The Suhara Foundation and The Kudo Science Foundation.

References

Aravind, L. and Koonin, E. V. (2000). The U box is a modified RING finger - a common domain in ubiquitination. *Curr. Biol.* **10**, R132-R134.

Bahram, F., von der Lehr, N., Cetinkaya, C. and Larsson, L. G. (2000). Myc hot spot mutations in lymphomas result in inefficient ubiquitination and decreased proteasome-mediated turnover. *Blood* **95**, 2104-2110.

Cartwright, P., McLean, C., Sheppard, A., Rivett, D., Jones, K. and Dalton, S. (2005). LIF/STAT3 controls ES cell self-renewal and pluripotency by a Myc-dependent mechanism. *Development* **132**, 885-896.

Chan, K. K., Zhang, J., Chia, N. Y., Chan, Y. S., Sim, H. S., Tan, K. S., Oh, S. K., Ng, H. H. and Choo, A. B. (2009). KLF4 and PBX1 directly regulate NANOG expression in human embryonic stem cells. *Stem Cells* **27**, 2114-2125.

Cyr, D. M., Hohfeld, J. and Patterson, C. (2002). Protein quality control: U-box-containing E3 ubiquitin ligases join the fold. *Trends Biochem. Sci.* **27**, 368-375.

Daksis, J. I., Lu, R. Y., Facchini, L. M., Marhin, W. W. and Penn, L. J. (1994). Myc induces cyclin D1 expression in the absence of de novo protein synthesis and links mitogen-stimulated signal transduction to the cell cycle. *Oncogene* **9**, 3635-3645.

Dang, C. V. (1999). Myc target genes involved in cell growth, apoptosis, and metabolism. *Mol. Cell. Biol.* **19**, 1-11.

Darr, H., Mayshar, Y. and Benvenisty, N. (2006). Overexpression of NANOG in human ES cells enables feeder-free growth while inducing primitive ectoderm features. *Development* **133**, 1193-1201.

Elbashir, S. M., Harborth, J., Weber, K. and Tuschl, T. (2002). Analysis of gene function in somatic mammalian cells using small interfering RNAs. *Methods* **26**, 199-213.

Freemont, P. S. (2000). RING for destruction? *Curr. Biol.* **10**, R84-R87.

Hatakeyama, S., Yada, M., Matsumoto, M., Ishida, N. and Nakayama, K. I. (2001). U box proteins as a new family of ubiquitin-protein ligases. *J. Biol. Chem.* **276**, 33111-33120.

Hershko, A. and Ciechanover, A. (1992). The ubiquitin system for protein degradation. *Annu. Rev. Biochem.* **61**, 761-807.

Hershko, A. and Ciechanover, A. (1998). The ubiquitin system. *Annu. Rev. Biochem.* **67**, 425-479.

Hershko, A., Heller, H., Elias, S. and Ciechanover, A. (1983). Components of ubiquitin-protein ligase system. Resolution, affinity purification, and role in protein breakdown. *J. Biol. Chem.* **258**, 8206-8214.

Hishida, T., Nozaki, Y., Nakachi, Y., Mizuno, Y., Okazaki, Y., Ema, M., Takahashi, S., Nishimoto, M. and Okuda, A. (2011). Indefinite self-renewal of ESCs through Myc/Max transcriptional complex-independent mechanisms. *Cell Stem Cell* **9**, 37-49.

Huibregtse, J. M., Scheffner, M., Beaudenon, S. and Howley, P. M. (1995). A family of proteins structurally and functionally related to the E6-AP ubiquitin-protein ligase. *Proc. Natl. Acad. Sci. USA* **92**, 2563-2567.

Joazeiro, C. A. and Weissman, A. M. (2000). RING finger proteins: mediators of ubiquitin ligase activity. *Cell* **102**, 549-552.

Kano, S., Miyajima, N., Fukuda, S. and Hatakeyama, S. (2008). Tripartite motif protein 32 facilitates cell growth and migration via degradation of Abl-interactor 2. *Cancer Res.* **68**, 5572-5580.

Kim, S. Y., Herbst, A., Tworkowski, K. A., Salghetti, S. E. and Tansey, W. P. (2003). Skp2 regulates Myc protein stability and activity. *Mol. Cell* **11**, 1177-1188.

Knoepfler, P. S., Cheng, P. F. and Eisenman, R. N. (2002). N-Myc is essential during neurogenesis for the rapid expansion of progenitor cell populations and the inhibition of neuronal differentiation. *Genes Dev.* **16**, 2699-2712.

Knofler, M., Meinhardt, G., Bauer, S., Loregger, T., Vasicek, R., Bloor, D. J., Kimber, S. J. and Husslein, P. (2002). Human Hand1 basic helix-loop-helix (bHLH) protein: extra-embryonic expression pattern, interaction partners and identification of its transcriptional repressor domains. *Biochem. J.* **361**, 641-651.

Kunath, T., Saba-El-Leil, M. K., Almousailleakh, M., Wray, J., Meloche, S. and Smith, A. (2007). FGF stimulation of the Erk1/2 signalling cascade triggers transition of pluripotent embryonic stem cells from self-renewal to lineage commitment. *Development* **134**, 2895-2902.

Kwon, G. S., Fraser, S. T., Eakin, G. S., Mangano, M., Isern, J., Sahr, K. E., Hadjantonakis, A. K. and Baron, M. H. (2006). TAfp-GFP) expression marks primitive and definitive endoderm lineages during mouse development. *Dev. Dyn.* **235**, 2549-2558.

Lorick, K. L., Jensen, J. P., Fang, S., Ong, A. M., Hatakeyama, S. and Weissman, A. M. (1999). RING fingers mediate ubiquitin-conjugating enzyme (E2)-dependent ubiquitination. *Proc. Natl. Acad. Sci. USA* **96**, 11364-11369.

Lutterbach, B. and Hann, S. R. (1994). Hierarchical phosphorylation at N-terminal transformation-sensitive sites in Myc protein is regulated by mitogens and in mitosis. *Mol. Cell. Biol.* **14**, 5510-5522.

Meroni, G. and Diez-Roux, G. (2005). TRIM/RBCC, a novel class of 'single protein RING finger' E3 ubiquitin ligases. *BioEssays* **27**, 1147-1157.

Miyajima, N., Maruyama, S., Bohgaki, M., Kano, S., Shigemura, M., Shinohara, N., Nonomura, K. and Hatakeyama, S. (2008). TRIM68 regulates ligand-dependent transcription of androgen receptor in prostate cancer cells. *Cancer Res.* **68**, 3486-3494.

Morita, S., Kojima, T. and Kitamura, T. (2000). Plat-E: an efficient and stable system for transient packaging of retroviruses. *Gene Ther.* **7**, 1063-1066.

Nakagawa, M., Koyanagi, M., Tanabe, K., Takahashi, K., Ichisaka, T., Aoi, T., Okita, K., Mochiduki, Y., Takizawa, N. and Yamanaka, S. (2008). Generation of induced pluripotent stem cells without Myc from mouse and human fibroblasts. *Nat. Biotechnol.* **26**, 101-106.

Nisole, S., Stoye, J. P. and Saib, A. (2005). TRIM family proteins: retroviral restriction and antiviral defence. *Nat. Rev. Microbiol.* **3**, 799-808.

Niwa, H., Burdon, T., Chambers, I. and Smith, A. (1998). Self-renewal of pluripotent embryonic stem cells is mediated via activation of STAT3. *Genes Dev.* **12**, 2048-2060.

Niwa, H., Miyazaki, J. and Smith, A. G. (2000). Quantitative expression of Oct-3/4 defines differentiation, dedifferentiation or self-renewal of ES cells. *Nat. Genet.* **24**, 372-376.

Niwa, H., Ogawa, K., Shimosato, D. and Adachi, K. (2009). A parallel circuit of LIF signalling pathways maintains pluripotency of mouse ES cells. *Nature* **460**, 118-122.

Okita, K., Nakagawa, M., Hyenjong, H., Ichisaka, T. and Yamanaka, S. (2008). Generation of mouse induced pluripotent stem cells without viral vectors. *Science* **322**, 949-953.

Okumura, F., Hatakeyama, S., Matsumoto, M., Kamura, T. and Nakayama, K. I. (2004). Functional regulation of FEZ1 by the U-box-type ubiquitin ligase E4B contributes to neuritogenesis. *J. Biol. Chem.* **279**, 53533-53543.

Ozato, K., Shin, D. M., Chang, T. H. and Morse, H. C., 3rd. (2008). TRIM family proteins and their emerging roles in innate immunity. *Nat. Rev. Immunol* **8**, 849-860.

Perez-Roger, I., Kim, S. H., Griffiths, B., Sewing, A. and Land, H. (1999). Cyclins D1 and D2 mediate Myc-induced proliferation via sequestration of p27(Kip1) and p21(Cip1). *EMBO J.* **18**, 5310-5320.

Peters, J. M. (1998). SCF and APC: the Yin and Yang of cell cycle regulated proteolysis. *Curr. Opin. Cell Biol.* **10**, 759-768.

Quaderi, N. A., Schweiger, S., Gaudenz, K., Franco, B., Rugarli, E. I., Berger, W., Feldman, G. J., Volta, M., Andolfi, G., Gilgenkrantz, S. et al. (1997). Opitz G/BBB syndrome, a defect of midline development, is due to mutations in a new RING finger gene on Xp22. *Nat. Genet.* **17**, 285-291.

Reymond, A., Meroni, G., Fantozzi, A., Merla, G., Cairo, S., Luzi, L., Riganelli, D., Zanaria, E., Messali, S., Cainarca, S. et al. (2001). The tripartite motif family identifies cell compartments. *EMBO J.* **20**, 2140-2151.

Satoh, Y., Matsumura, I., Tanaka, H., Ezoe, S., Sugahara, H., Mizuki, M., Shibayama, H., Ishiko, E., Ishiko, J., Nakajima, K. et al. (2004). Roles for Myc in self-renewal of hematopoietic stem cells. *J. Biol. Chem.* **279**, 24986-24993.

Scheffner, M., Nuber, U. and Huibregtse, J. M. (1995). Protein ubiquitination involving an E1-E2-E3 enzyme ubiquitin thioester cascade. *Nature* **373**, 81-83.

Soudais, C., Bielinska, M., Heikinheimo, M., MacArthur, C. A., Narita, N., Saffitz, J. E., Simon, M. C., Leiden, J. M. and Wilson, D. B. (1995). Targeted mutagenesis of the transcription factor GATA-4 gene in mouse embryonic stem cells disrupts visceral endoderm differentiation in vitro. *Development* **121**, 3877-3888.

Takahashi, K. and Yamanaka, S. (2006). Induction of pluripotent stem cells from mouse embryonic and adult fibroblast cultures by defined factors. *Cell* **126**, 663-676.

Takayama, N., Nishimura, S., Nakamura, S., Shimizu, T., Ohnishi, R., Endo, H., Yamaguchi, T., Otsu, M., Nishimura, K., Nakanishi, M. et al. (2010). Transient activation of Myc expression is critical for efficient platelet generation from human induced pluripotent stem cells. *J. Exp. Med.* **207**, 2817-2830.

Tian, L., Wu, X., Lin, Y., Liu, Z., Xiong, F., Han, Z., Zhou, Y., Zeng, Q., Wang, Y., Deng, J. et al. (2009). Characterization and potential function of a novel pre-implantation embryo-specific RING finger protein: TRIML1. *Mol. Reprod Dev.* **76**, 656-664.

Tropepe, V., Hitoshi, S., Sirard, C., Mak, T. W., Rossant, J. and van der Kooy, D. (2001). Direct neural fate specification from embryonic stem cells: a primitive mammalian neural stem cell stage acquired through a default mechanism. *Neuron* **30**, 65-78.

van Riggelen, J., Yetil, A. and Felsher, D. W. (2010). MYC as a regulator of ribosome biogenesis and protein synthesis. *Nat. Rev. Cancer* **10**, 301-309.

von der Lehr, N., Johansson, S., Wu, S., Bahram, F., Castell, A., Cetinkaya, C., Hydbring, P., Weidung, I., Nakayama, K., Nakayama, K. I. et al. (2003). The F-box protein Skp2 participates in Myc proteosomal degradation and acts as a cofactor for Myc-regulated transcription. *Mol. Cell* **11**, 1189-1200.

Watanabe, S., Umehara, H., Murayama, K., Okabe, M., Kimura, T. and Nakano, T. (2006). Activation of Akt signaling is sufficient to maintain pluripotency in mouse and primate embryonic stem cells. *Oncogene* **25**, 2697-2707.

Watt, F. M., Frye, M. and Benitah, S. A. (2008). Myc in mammalian epidermis: how can an oncogene stimulate differentiation? *Nat. Rev. Cancer* **8**, 234-242.

Wilson, A., Murphy, M. J., Oskarsson, T., Kaloulis, K., Bettess, M. D., Oser, G. M., Pasche, A. C., Knabenhans, C., Macdonald, H. R. and Trumpp, A. (2004). Myc controls the balance between hematopoietic stem cell self-renewal and differentiation. *Genes Dev.* **18**, 2747-2763.

Yada, M., Hatakeyama, S., Kamura, T., Nishiyama, M., Tsunematsu, R., Imaki, H., Ishida, N., Okumura, F., Nakayama, K. and Nakayama, K. I. (2004). Phosphorylation-dependent degradation of Myc is mediated by the F-box protein Fbw7. *EMBO J.* **23**, 2116-2125.

Ying, Q. L., Wray, J., Nichols, J., Batlle-Morera, L., Doble, B., Woodgett, J., Cohen, P. and Smith, A. (2008). The ground state of embryonic stem cell self-renewal. *Nature* **453**, 519-523.

Gene 497 (2012) 110–115

Contents lists available at SciVerse ScienceDirect

Gene

journal homepage: www.elsevier.com/locate/gene

Short Communication

Somatic mosaicism in two unrelated patients with X-linked chronic granulomatous disease characterized by the presence of a small population of normal cells

Masafumi Yamada [a,*], Yuka Okura [a], Yasuto Suzuki [b], Shinobu Fukumura [c], Toru Miyazaki [d], Hisami Ikeda [d], Shun-Ichiro Takezaki [a], Nobuaki Kawamura [a], Ichiro Kobayashi [a], Tadashi Ariga [a]

[a] Department of Pediatrics, Hokkaido University Graduate School of Medicine, Sapporo, 060-8638, Japan
[b] Department of Pediatrics, Kushiro Red Cross Hospital, Kushiro, 085-8512, Japan
[c] Department of Pediatrics, Kushiro City General Hospital, Kushiro, 085-0822, Japan
[d] Hokkaido Red Cross Blood Center, Sapporo, 063-0002, Japan

ARTICLE INFO

Article history:
Accepted 17 January 2012
Available online 28 January 2012

Keywords:
X-linked chronic granulomatous disease (X-CGD)
Cytochrome b_{558} *β (CYBB)*
Somatic mosaicism
De novo mutation
Reversion

ABSTRACT

X-linked chronic granulomatous disease (X-CGD) is a primary immunodeficiency disease of phagocytes caused by mutations in the *cytochrome* b_{558} *β (CYBB)* gene. We, for the first time, detected somatic mosaicism in two unrelated male patients with X-CGD caused by *de novo* nonsense mutations (p.Gly223X and p.Glu462X) in the *CYBB* gene. In each patient, a small subset of granulocytes was normal in terms of respiratory burst (ROB) activity, $gp91^{phox}$ expression, and *CYBB* sequences. Cells with wild-type *CYBB* sequence were also detected in buccal swab specimens and in peripheral blood mononuclear cells. The normal cells were shown to be of the patient origin by fluorescent *in situ* hybridization analysis of X/Y chromosomes, and by HLA DNA typing. Two possible mechanisms for this somatic mosaicism were considered. The first is that the *de novo* disease-causing mutations in *CYBB* occurred at an early multicellular stage of embryogenesis with subsequent expansion of the mutated cells, leaving some unmutated cells surviving. The second possibility is that the *de novo* mutations occurred in oocytes which was followed by reversion of the mutations in a small subset of cells in early embryogenesis.

1. Introduction

Chronic granulomatous disease (CGD) is a primary immunodeficiency disease (PID) caused by mutations in one of five genes encoding subunits of the nicotinamide dinucleotide phosphate (NADPH) oxidase complex, leading to defective production of superoxide and other reactive oxygen species in phagocytic cells (Malech and Gallin, 1987; Matute et al., 2009). The most common form is X-linked recessive CGD (X-CGD), which results from mutations in the *cytochrome* b_{558} *β (CYBB)* gene encoding $gp91^{phox}$ (Winkelstein et al., 2000).

Somatic mosaicism has recently been identified in various genetic diseases. This mosaicism can be due to *de novo* mutations that occur during embryogenesis, or to reversion of inherited mutations (Hirschhorn, 2003). The former is associated with highly variable mosaicism and may be accompanied by germ line mosaicism depending on the stage of embryogenesis in which the mutation occurs (Frank, 2010; Hirschhorn, 2003). The latter has been reported in several disorders, including PIDs, in which the reversion gives a growth advantage to the corrected cells (Hirschhorn, 2003). The critical difference is that it can be shown that the mutation that reverted to normal had been inherited from a parent (Hirschhorn, 2003).

In this study, we, for the first time, have demonstrated somatic mosaicism in two unrelated male patients with X-CGD caused by *de novo* nonsense mutations in the *CYBB* gene.

2. Materials and methods

2.1. Patients

Patient 1 was a 13-year-old male born to non-consanguineous Japanese parents. At birth, he had preaxial polydactyly of the right hand. He had borderline developmental delay noticed at the age of 5 months. Recurrent perianal abscesses and lymphadenitis led to the diagnosis of X-CGD at the age of 1 year. He mistakenly received BCG vaccination at the age of 7 years without significant complications, with a prophylactic treatment with isoniazid for 6 months. He developed a liver abscess at the age of 12 years which required surgical

Abbreviations: X-CGD, X-linked chronic granulomatous disease; *CYBB, cytochrome* b_{558} *β*; ROB, respiratory burst; PBMC, peripheral blood mononuclear cells; PID, primary immunodeficiency disease; EBV-LCLs, EBV-transformed lymphoblastoid cell lines.

* Corresponding author at: Department of Pediatrics, Hokkaido University Graduate School of Medicine, North 15 West 7, Kita-ku Sapporo, 060-8638, Japan. Tel.: +81 11 706 5954; fax: +81 11 7067898.
E-mail address: yamadam@med.hokudai.ac.jp (M. Yamada).

0378-1119/$ – see front matter © 2012 Elsevier B.V. All rights reserved.
doi:10.1016/j.gene.2012.01.019

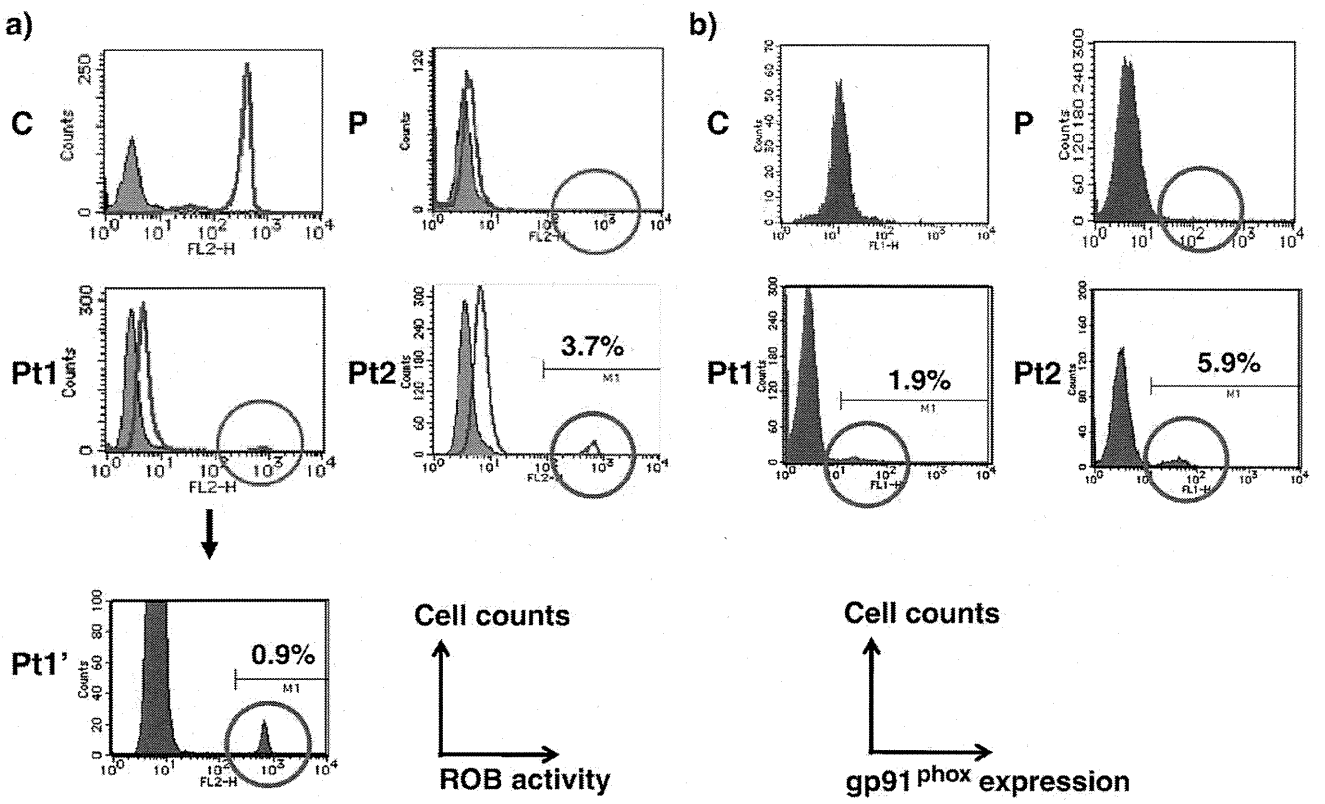

Fig.1. Respiratory burst (ROB) analysis and surface gp91^{phox} expression in granulocytes. (a) ROB analysis of granulocytes left unstimulated (filled orange) or stimulated with phorbol myristate acetate (empty blue). (b) Granulocyte surface gp91^{phox} expression. C: a normal control, P: a typical X-CGD patient, Pt1: Patient 1, Pt1': An enlarged view of Patient 1's ROB result, Pt2: Patient 2.

resection. Patient 2 was a 2-year-old male with a history of BCG lymphadenitis at the age of 1 year, which was controlled by treatment with isoniazid for 6 months. He developed persistent diarrhea with liver dysfunction at the age of 2 years, which was controlled by oral steroid treatment. Both patients have no history of transfusion.

2.2. Flow cytometric analysis of granulocyte respiratory burst (ROB) activity and surface gp91^{phox} expression

These analyses were performed following the methods described elsewhere (Yamada et al., 2000).

2.3. Enrichment of gp91^{phox} + cells

Granulocytes were first Fc-blocked with the patient's own serum to avoid possible contamination of the cells by foreign DNA from commercially obtained AB sera. The cells were reacted with monoclonal mouse anti-gp91^{phox} antibody, 7D5 provided by Dr. M. Nakamura, washed three times, then reacted with anti-mouse IgG1 conjugated with magnetic beads (Miltenyi Biotec, Auburn CA, USA). The enriched population of gp91^{phox}+cells was obtained by positive selection with MACS sorting (Miltenyi Biotec).

2.4. Studies of direct sequencing and TA clones of CYBB

Informed consent for genetic analysis was obtained from the patients, their mothers, and normal controls under a protocol approved by the Institutional Review Board (IRB) of Hokkaido University Hospital. Genomic DNA was extracted from heparinized blood or buccal swab samples using SepaGene (Sankojunyaku, Tokyo, Japan). PCR and sequencing conditions were described elsewhere (Ariga et al., 1998). PCR primers used for genomic DNA were located in the flanking regions of each exon in *CYBB* as reported (Hui et al., 1997). Nucleotide number 1 corresponds to the A of the ATG translation–initiation codon. The presence of wild-type sequences was confirmed by sequencing TA clones obtained with the TOPO-TA cloning kit (Invitrogen, Carlsbad, CA, USA) following the manufacturer's instructions.

2.5. Generation of EBV-transformed cell lines (EBV-LCLs)

EBV-LCLs were generated by *in vitro* transformation of human B cells with EBV (strain B95-8), as described elsewhere (Tosato and Cohen, 2007).

2.6. HLA DNA typing study

This study was performed following the methods described elsewhere (Ariga et al., 2001a, 2001b). Briefly, DNA typing for identification of HLA class I alleles was performed by PCR-SSOP (Sequence Specific Oligonucleotide Probe) with Luminex 100 xMAP flow cytometry dual-laser system to quantitate fluorescently labeled oligonucleotides attached to color-coded microbeads. Type of HLA class I was determined using WAKFlow HLA Typing (purchased from Wakunaga Pharmaceutical, Hiroshima, Japan).

2.7. Monocyte-derived macrophages and dendritic cells

Isolated peripheral blood mononuclear cells (PBMC) were seeded in a 6-well culture plate at a density of 5×10^6/ml. After incubation at 37 °C in a 5% CO_2 incubator for an hour, nonadherent cells were removed with vigorous pipetting with prewarmed RPMI1640 to obtain adherent monocytes. The adherent monocytes were then differentiated

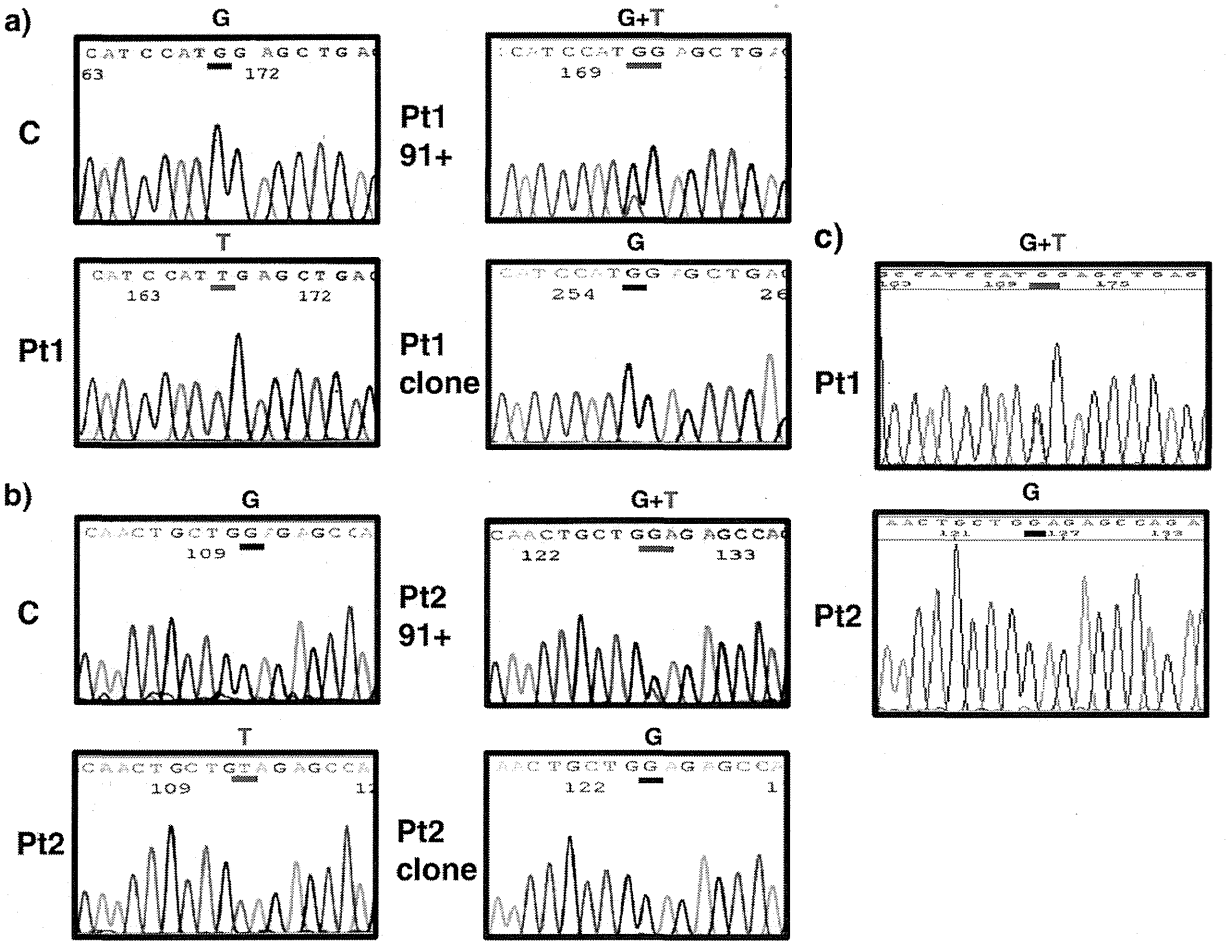

Fig. 2. Sequence analysis of the *CYBB* gene. (a) Sequence analysis of *CYBB* exon 6 in Patient 1. (b) Sequence analysis of *CYBB* exon 11 in Patient 2. (c) Sequence analysis of *CYBB* exon 6 and exon 11 in EBV-LCLs from Patient 1 (Pt1) and Patient 2 (Pt2), respectively. C: a control. Pt1: Patient 1. Pt2: Patient 2. 91+: gp91^{phox}-enriched granulocytes. Clone: a TA clone with wild-type sequence.

into macrophages by culturing for 7 days in RPMI1640 containing 10% fetal bovine serum in the presence of 5 ng/ml of GM-CSF (R&D, Minneapolis, MN) or 10 ng/ml of M-CSF (R&D). They were also differentiated into dendritic cells by culturing in the presence of 5 ng/ml of GM-CSF + 5 ng/ml of IL-4 (R&D) or 5 ng/ml of GM-CSF + 1500 units/ml of IFN-α (Biosource International, Camarillo, CA) for 7 days.

3. Results

A small subset of granulocytes was reproducibly shown to have normal ROB activity in both Patient 1 and Patient 2, while the majority of the cells had deficient activity (Fig. 1a). Normal surface gp91^{phox} expression was also reproducibly detected in a small subset of granulocytes from both patients (Fig. 1b), indicating that the granulocytes with normal ROB activity were gp91^{phox}-positive. Subsets of cells with normal ROB activity or normal surface gp91^{phox} expression were not detected in 10 other X-CGD patients studied (Figs. 1a, b, and data not shown). Direct sequence analysis of the *CYBB* gene using genomic DNA from whole blood cells demonstrated a novel c.667 G>T (p.Gly223X) mutation in exon 6 in Patient 1 (Fig. 2a) and a previously reported c.1384 G>T (p.Glu462X) mutation in exon 11 in Patient 2 (Fig. 2b) (Gérard et al., 2001). Mothers of the two patients had only the wild-type sequences of *CYBB* (data not shown), indicating that both patients had *de novo* mutations. However, wild-type sequences at the mutation sites were detected by direct sequencing of PCR products from genomic DNA from both patients after gp91^{phox}-positive granulocytes were enriched with MACS sorting (Figs. 2a and b). The presence of the wild-type sequences was confirmed by sequence analysis of TA clones obtained from gp91^{phox}-positive granulocytes (Figs. 2a and b). These results indicate that a small subset of granulocytes in both patients have the wild-type *CYBB* sequence. Wild-type TA clones of PCR products from genomic DNA were also detected in unselected granulocyte, PBMC, and buccal swab samples from Patient 2, and from a buccal swab sample from Patient 1 (Table 1).

We then studied gp91^{phox} expression and *CYBB* sequences in EBV-LCLs, which are also known to express gp91^{phox}. Although a gp91^{phox}-positive population in EBV-LCLs was not detected 3 weeks after EBV infection, but was detected in a small subset 2 months after its infection in both patients (Fig. 3). This subset, for unknown reasons, was greater

Table 1
Summary of the proportion of granulocytes with normal ROB activity and the proportion of clones with wild-type CYBB sequence in various samples from the two patients.

	Patient 1	Patient 2
ROB + granulocytes	0.9%	3.7%
Wild-type *CYBB* clones		
Granulocytes	0% (0/211)	7.3% (4/55)
PBMC	0% (0/52)	1.6% (1/61)
Buccal swab	1.8% (2/109)	18.8% (6/32)

The fraction in each parenthesis indicates the number of wild-type clones out of the total number of clones analyzed for each sample.

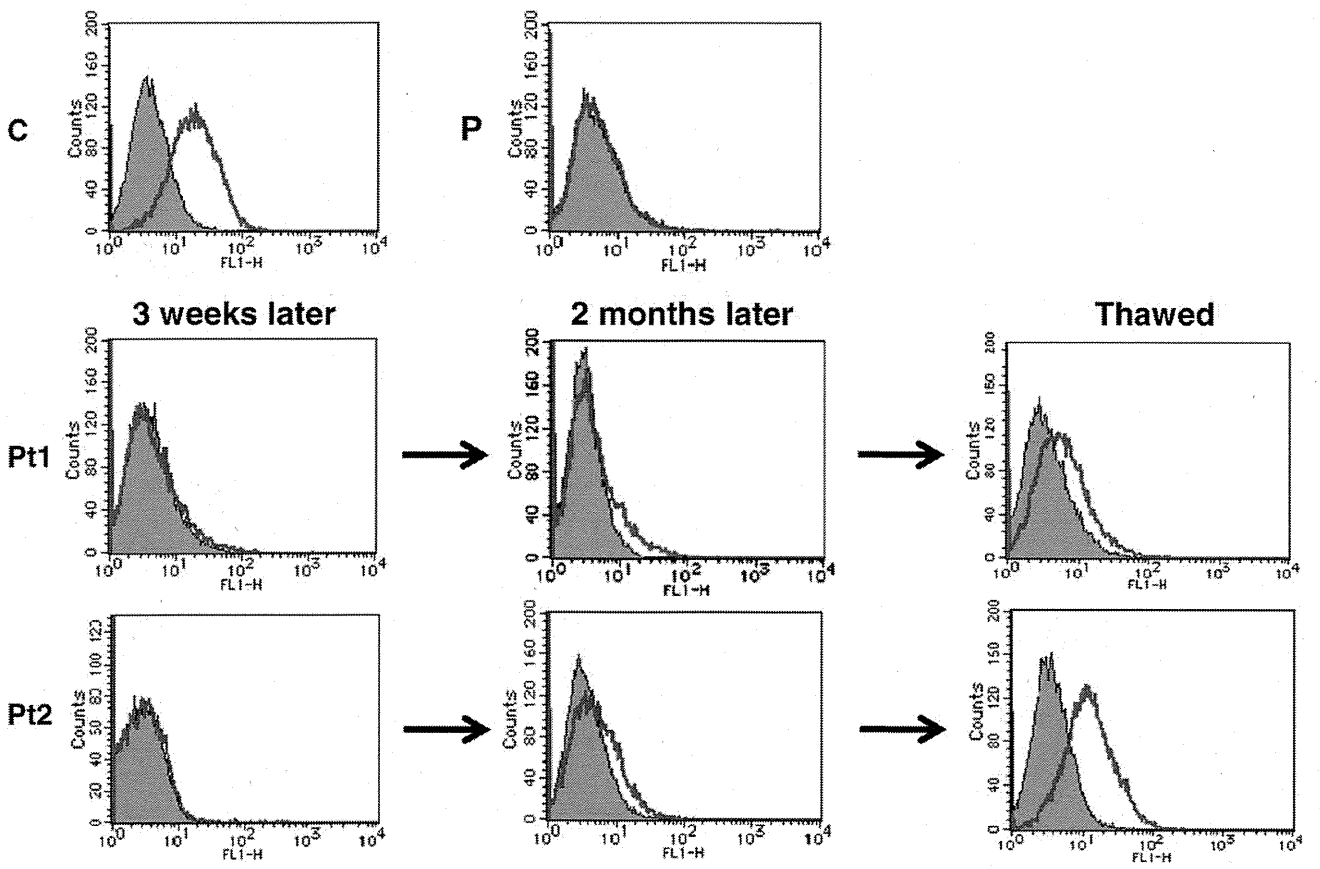

Fig. 3. Surface gp91^{phox} expression in EBV-LCLs 3 weeks and 2 months after EBV infection (3 weeks later and 2 months later). We also studied its expression after thawing the freeze-stored cell lines. Filled orange: isotypic control (mouse IgG1), Empty blue: gp91^{phox} expression.

in some of the EBV-LCLs which were thawed from the freeze-stored original cell lines (Fig. 3 and data not shown). According to the intensity of the wild-type sequence signals, this population was estimated to be about 50% in Patient 1 and 100% in Patient 2, respectively (Fig. 2c).

To exclude the possibility that the normal cells observed in both patients were due to maternal cell engraftment, fluorescent *in situ* hybridization (FISH) analysis of chromosomes X and Y and HLA DNA typing study were performed. FISH analysis in whole blood cells from both patients showed only the XY karyotype in 500 analyzed cells (data not shown). HLA DNA typing also showed only the patients' HLA types of HLA-A*1101, HLA-A*2402, HLA-B*1301, and HLA-B*4002 in enriched gp91^{phox}-positive granulocytes and EBV-LCLs described in Fig. 2c (Table 2). These results indicate that the normal cells were of the patient origin.

CYBB mutations that selectively affect macrophages were recently reported to predispose patients to tuberculous mycobacterial disease (Bustamante et al., 2011), suggesting human tissue macrophages are critical for immunity at least to tuberculosis. To estimate the normal population in tissue macrophages and to study the possibility of selectively expanding the normal population with cytokines, we studied gp91^{phox} expression in monocyte-derived macrophages from Patient 2. Monocyte-derived dendritic cells were also studied. After 7 days of culture, monocytes morphologically changed into macrophages in the presence of GM-CSF or M-CSF, and into dendritic cells in the presence of GM-CSF + IL-4 or GM-CSF + IFNα. The differentiated cells were harvested for the analysis of surface gp91^{phox} expression. Macrophages from normal individuals differentiated with GM-CSF or M-CSF, and dendritic cells differentiated with GM-CSF + IFNα were shown to have surface gp91^{phox} expression comparable to undifferentiated monocytes, while dendritic cells from the normal individuals differentiated with GM-CSF + IL-4 lost its surface expression (data not shown). In Patient 2, the proportions of gp91^{phox} + cells in macrophages differentiated with GM-CSF or M-CSF, and in dendritic cells differentiated with GM-CSF + IFNα, were not significantly different from that of undifferentiated monocytes (Fig. 4).

4. Discussion

This study demonstrates the presence of somatic mosaicism in two unrelated X-CGD patients with *de novo* nonsense mutations in the *CYBB* gene. A small subset of normal cells was found to be present in granulocytes, buccal swab samples, EBV-LCLs, and/or PBMC from both patients.

Somatic mosaicism can result from *de novo* mutations during embryogenesis or from reversion of inherited mutations (Hirschhorn,

Table 2
Results of HLA DNA typing in granulocytes and EBV-LCL.

Sample	A*	A*	B*	B*
Patient 1 granulocytes	1101 (11)	2402 (24)	1301 (13)	4002 (61)
Patient 1 EBV-LCL	1101 (11)	2402 (24)	1301 (13)	4002 (61)
Patient 1's mother granulocytes	2402 (24)	2603 (26)	3501 (35)	4002 (61)
Patient 2 granulocytes	3101 (31)	3303 (33)	4403 (44)	5101 (51)
Patient 2 EBV-LCL	3101 (31)	3303 (33)	4403 (44)	5101 (51)
Patient 2's mother granulocytes	0206 (2)	3303 (33)	4006 (61)	4403 (44)

Enriched gp91^{phox}-positive granulocytes and EBV-LCL were studied for Patient 1 and Patient 2.
( ) : Serotype.

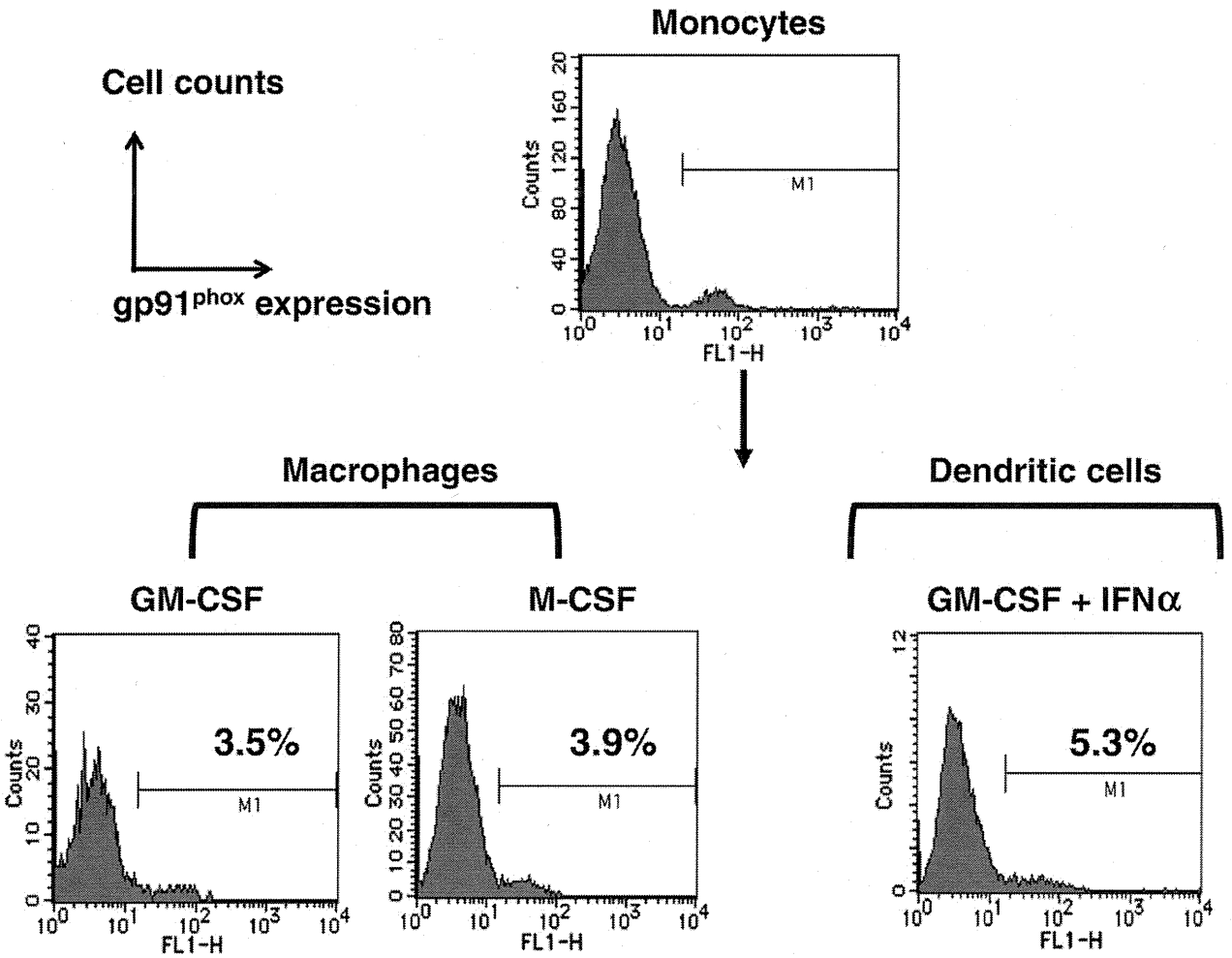

Fig. 4. Surface gp91^{phox} expression in monocytes and monocyte-derived macrophages and dendritic cells in Patient 2. Monocytes were differentiated into macrophages and dendritic cells by the cytokines indicated above each histogram.

2003). A *de novo* mutation could make a significant contribution to the fetus if the mutation occurred at an early stage of embryogenesis, when only a few cells contribute to the embryo (Erickson, 2010). A mutation during embryogenesis may also result in germ line mosaicism depending on the stage of embryogenesis in which the mutation occurs (Frank, 2010; Hirschhorn, 2003). On the other hand, the reversion of inherited mutations has been reported in some disorders, including several PIDs, when the reversion gives a growth advantage to the corrected cells (Hirschhorn, 2003). In these cases the mutation that has reverted to normal has been inherited from a parent (Hirschhorn, 2003).

Considering that the *CYBB* mutations were not detected in their mothers, it is likely that the *de novo* mutations occurred in the patients at an early multicellular stage of embryogenesis with subsequent expansion of the mutated cells, leaving some unmutated cells surviving. This mechanism may also explain the presence of a normal population in various cell lineages as observed in the present patients, since most of the stem cells could carry a mutation when the mutation arises in pluripotent stem cells at an early stage of embryogenesis (Frank, 2010). It might be also possible that the mutations had occurred in oogenesis, and were reverted to normal in a small subset of cells in early embryogenesis. Additionally, we have not completely ruled out the possibility that their mothers have germ line mosaicism and the patients had reversion to normal of inherited mutations in a small subset of cells, although the patients have not had siblings who share the same mutations. In any case, it was not determined whether somatic mosaicism observed in the patients was accompanied by germ line mosaicism in this study.

Somatic mosaicism was observed in leukocytes from an adult female who showed unusual late presentation of X-CGD (Wolach et al., 2005). In contrast, there have been no previous reports of somatic mosaicism in male patients with X-CGD that has been defined at the molecular level, although X-CGD is one of the most common PIDs. Reports of mosaicism in X-CGD may be rare because of the difficulty of detecting a small population of normal cells. Unmutated (revertant) normal cells may have no growth advantage over mutated cells. In fact, Patient 1 was retrospectively shown to have 0.5–1% of granulocytes with normal ROB activity at the age of 3 and 11 years, which had been overlooked until this study. Another possibility is that somatic mosaicism, regardless of its mechanism, is very rare in X-CGD. There is one report of three adult males in two kindreds with X-CGD that was inherited from their mothers, who were shown to have 5–15% of neutrophils and monocytes with normal ROB activity (Woodman et al., 1995). It is possible that these are X-CGD patients with somatic mosaicism, due to reversion of maternally inherited mutations, but the molecular characteristics of the normal cells were not determined in this study, nor was it shown that the normal cells were of patient and not maternal origin.

Somatic mosaicism may have some effects on the clinical phenotype in patients with other PIDs (Ariga et al., 2001a, 2001b; Stephan et al., 1996; Tone et al., 2007; Wada et al., 2001). In X-CGD, based

on studies of female carriers with skewed X-inactivation (Lun et al., 2002; Rösen-Wolff et al., 2001; Wolach et al., 2005), it is estimated that if more than 5–10% of granulocytes are normal, there is much less susceptibility to infection. In Patient 1, a low fraction (<1%) of normal granulocytes had been stably present since the age of 3 years, but he developed liver abscesses at the age of 12 years. This indicates that his clinical course had not been, and probably will not be, modified by the presence of the normal cells. In contrast, Patient 2 might expect some clinical benefit from the normal cells, which were more abundant. It is uncertain whether the normal cell populations in these patients will increase over time. The results of our *in vitro* studies of expanding the normal population have been discouraging (Fig. 3), but these studies focused on the monocytic cells, and not on the granulocytes, which in any case are terminally differentiated. We need to observe if an expansion of the normal granulocytes or monocytes occurs over time *in vivo* which could be correlated with the improvement of clinical phenotypes.

Conflict of interest statement

The authors have no financial conflicts of interest.

Acknowledgments

This work was supported in part by a grant for Research on Intractable Diseases from the Japanese Ministry of Health, Labor and Welfare. We thank Dr. Nakamura M for providing us with monoclonal mouse anti-gp91^{phox} antibody, 7D5. And we thank Dr. Stewart DM for reviewing the manuscript.

References

Ariga, T., et al., 1998. Genetic analysis of 13 families with X-linked chronic granulomatous disease reveals a low proportion of sporadic patients and a high proportion of sporadic carriers. Pediatr. Res. 44, 85–92.

Ariga, T., et al., 2001a. T-cell lines from 2 patients with adenosine deaminase (ADA) deficiency showed the restoration of ADA activity resulted from the reversion of an inherited mutation. Blood 97, 2896–2899.

Ariga, T., et al., 2001b. Spontaneous in vivo reversion of an inherited mutation in the Wiskott-Aldrich syndrome. J. Immunol. 166, 5245–5249.

Bustamante, J., et al., 2011. Germline CYBB mutations that selectively affect macrophages in kindreds with X-linked predisposition to tuberculous mycobacterial disease. Nat. Immunol. 12, 213–221.

Erickson, R.P., 2010. Somatic gene mutation and human disease other than cancer: an update. Mutat. Res. 705, 96–106.

Frank, S.A., 2010. Somatic evolutionary genomics: Mutations during development cause highly variable genetic mosaicism with risk of cancer and neurodegeneration. Proc. Natl. Acad. Sci. U. S. A. 107, 1725–1730.

Gérard, B., et al., 2001. Characterization of 11 novel mutations in the X-linked chronic granulomatous disease (CYBB gene). Hum. Mutat. 18, 163–166.

Hirschhorn, R., 2003. In vivo reversion to normal of inherited mutations in humans. J. Med. Genet. 40, 721–728.

Hui, Y.F., et al., 1997. Identification of mutations in seven Chinese patients with X-linked chronic granulomatous disease. Blood 88, 4021–4028.

Lun, A., et al., 2002. Unusual late onset of X-linked chronic granulomatous disease in an adult woman after unsuspicious childhood. Clin. Chem. 48, 780–781.

Malech, H.L., Gallin, J.I., 1987. Current concepts: immunology. Neutrophils in human diseases. N. Engl. J. Med. 317, 687–694.

Matute, J.D., et al., 2009. A new genetic subgroup of chronic granulomatous disease with autosomal recessive mutations in p40^{phox} and selective defects in neutrophil NADPH oxidase activity. Blood 114, 3309–3315.

Rösen-Wolff, A., et al., 2001. Increased susceptibility of a carrier of X-linked chronic granulomatous disease (CGD) to *Aspergillus fumigatus* infection associated with age-related skewing of lyonization. Ann. Hematol. 80, 113–115.

Stephan, V., et al., 1996. Atypical X-linked severe combined immunodeficiency due to possible spontaneous reversion of the genetic defect in T cells. N. Engl. J. Med. 335, 1563–1567.

Tone, Y., et al., 2007. Somatic revertant mosaicism in a patient with leukocyte adhesion deficiency type 1. Blood 109, 1182–1184.

Tosato, G., Cohen, J. I., 2007. Generation of Epstein-Barr Virus (EBV)-immortalized B cell lines. Curr. Protoc. Immunol. 76, 7.22.1–7.22.4.

Wada, T., et al., 2001. Somatic mosaicism in Wiskott–Aldrich syndrome suggests *in vivo* reversion by a DNA slippage mechanism. Proc. Natl. Acad. Sci. U. S. A. 98, 8697–8702.

Winkelstein, J.A., et al., 2000. Chronic granulomatous disease. Report on a national registry of 368 patients. Medicine (Baltimore) 79, 155–169.

Wolach, B., et al., 2005. Unusual late presentation of X-linked chronic granulomatous disease in an adult female with a somatic mosaic for a novel mutation in CYBB. Blood 105, 61–66.

Woodman, R.C., et al., 1995. A new X-linked variant of chronic granulomatous disease characterized by the existence of a normal clone of respiratory burst-competent phagocytic cells. Blood 85, 231–241.

Yamada, M., et al., 2000. Genetic studies of three Japanese patients with p22-phox-deficient chronic granulomatous disease: detection of a possible common mutant CYBA allele in Japan and a genotype-phenotype correlation in these patients. Br. J. Haematol. 108, 511–517.

ORIGINAL ARTICLE CLINICAL IMMUNOLOGY

Clinical features and outcome of X-linked lymphoproliferative syndrome type 1 (SAP deficiency) in Japan identified by the combination of flow cytometric assay and genetic analysis

Hirokazu Kanegane[1], Xi Yang[1], Meina Zhao[1], Kazumi Yamato[2], Masami Inoue[3], Kazuko Hamamoto[4], Chie Kobayashi[5,6], Ako Hosono[7], Yoshikiyo Ito[8], Yozo Nakazawa[9], Kiminori Terui[10], Kazuhiro Kogawa[11], Eiichi Ishii[12], Ryo Sumazaki[6] & Toshio Miyawaki[1]

[1]Department of Pediatrics, Graduate School of Medicine, University of Toyama, Toyama, Japan; [2]Department of Pediatrics, Graduate School of Medicine, Osaka City University, Osaka, Japan; [3]Department of Hematology/Oncology, Osaka Medical Center and Research Institute for Maternal and Child Health, Izumi, Japan; [4]Department of Pediatrics, Hiroshima Red Cross Hospital and Atomic-bomb Survivors Hospital, Hiroshima, Japan; [5]Department of Pediatrics, Ibaraki Children's Hospital, Mito, Japan; [6]Department of Child Health, Institute of Clinical Medicine, University of Tsukuba, Tsukuba, Japan; [7]Department of Pediatrics, National Cancer Center Hospital, Tokyo, Japan; [8]Department of Hematology, Harasanshin Hospital, Fukuoka, Japan; [9]Department of Pediatrics, Shinshu University Graduate School of Medicine, Matsumoto, Japan; [10]Department of Pediatrics, Hirosaki University Graduate School of Medicine, Hirosaki, Japan; [11]Department of Pediatrics, National Defense Medical College, Tokorozawa, Japan; [12]Department of Pediatrics, Ehime University Graduate School of Medicine, Toon, Japan

To cite this article: Kanegane H, Yang Xi, Zhao M, Yamato K, Inoue M, Hamamoto K, Kobayashi C, Hosono A, Ito Y, Nakazawa Y, Terui K, Kogawa K, Ishii E, Sumazaki R, Miyawaki T. Clinical features and outcome of X-linked lymphoproliferative syndrome type 1 (SAP deficiency) in Japan identified by the combination of flow cytometric assay and genetic analysis. *Pediatric Allergy Immunology* 2012: **23**: 488–493.

Keywords
flow cytometry; genetic analysis; hematopoietic stem cell transplantation; SLAM-associated protein; X-linked lymphoproliferative syndrome

Correspondence
Hirokazu Kanegane, Department of Pediatrics, Graduate School of Medicine, University of Toyama, 2630 Sugitani, Toyama, Toyama 930-0194, Japan
Tel.: 81 76 434 7313
Fax: 81 76 434 5029
E-mail: kanegane@med.u-toyama.ac.jp

Accepted for publication 18 January 2012

DOI:10.1111/j.1399-3038.2012.01282.x

Abstract

Objective: X-linked lymphoproliferative syndrome (XLP) type 1 is a rare immunodeficiency, which is caused by mutations in *SH2D1A* gene. The prognosis of XLP is very poor, and hematopoietic stem cell transplantation (HSCT) is the only curative therapy. We characterized the clinical features and outcome of Japanese patients with XLP-1.

Methods: We used a combination of flow cytometric analysis and genetic analysis to identify XLP-1 and reviewed the patient characteristics and survival with HSCT.

Results: We identified 33 patients from 21 families with XLP-1 in Japan. Twenty-one of the patients (65%) who did not undergo a transplant died of the disease and complications. Twelve patients underwent HSCT, and 11 of these (92%) survived.

Conclusion: We described the clinical characteristics and outcomes of Japanese patients with XLP-1, and HSCT was the only curative therapy for XLP-1. The rapid and accurate diagnosis of XLP with the combination of flow cytometric assay and genetic analysis is important.

X-linked lymphoproliferative syndrome (XLP) is a rare inherited immunodeficiency estimated to affect approximately one in one million males, although it may be under-diagnosed (1). XLP is characterized by extreme vulnerability to Epstein–Barr virus (EBV) infection, and the major clinical phenotypes of XLP include fulminant infectious mononucleosis (FIM) or EBV-associated hemophagocytic lymphohistiocytosis (HLH) (60%), lymphoproliferative disorder (30%), and dysgammaglobulinemia (30%) (2). In addition, XLP is associated with a variety of other clinical manifestations including vasculitis, aplastic anemia, and pulmonary lymphoid granulomatosis. Patients with XLP often develop more than one phenotype over time.

The responsible gene was first identified as *SH2D1A/SLAM-associated protein (SAP)* located in the region of Xq25 (3–5). However, some of the presumed patients with

XLP do not harbor *SH2D1A* mutations, although they are clinically and even histologically similar to XLP patients with *SH2D1A* mutations. A second causative gene that encodes X-linked inhibitor of apoptosis protein (XIAP), namely *XIAP* or *BIRC4* gene, has been identified (6). Patients with XLP-2 (XIAP deficiency) sometimes present with splenomegaly and hemorrhagic colitis, but no lymphoma. The *SH2D1A* and *XIAP* genes are close together at Xq25, but the molecular pathogenesis and clinical features of these diseases seem to be distinct (7, 8).

The vast majority of patients with XLP die in childhood; the survival rate is very poor, even with treatment (2). Hematopoietic stem cell transplantation (HSCT) is the only curative therapy for XLP (9, 10). Therefore, rapid definitive diagnosis and immediate treatment are extremely significant for better prognosis and survival of patients with XLP. We previously established the anti-SAP monoclonal antibody (mAb) and applied it to flow cytometric diagnosis of patients with XLP-1 (11). We performed a nationwide survey for XLP-1 with the flow cytometric assay and genetic analysis and identified a total of 33 patients from 21 families with XLP-1 in Japan (11–15). In this study, we elucidated the clinical and genetic characteristics of these patients. Twelve patients with XLP-1 underwent HSCT, and 11 of these (92%) survived. We also describe the outcomes of HSCT in Japan.

Materials and methods

Study subjects

The subjects in this study were largely male patients with FIM or EBV–HLH treated until the end of 2011. In addition, a few male patients with lymphoma or hypogammaglobulinemia with unknown genetic origin were suspected of having XLP. After written informed consent was obtained, 5–10 ml of venous blood was collected into heparin-containing syringes and delivered to the laboratory. Patients and families provided informed consent for genetic analyses in accordance with the 1975 Declaration of Helsinki, and the study protocol was approved by the Ethics Committee of the University of Toyama. Several patients were described in our previous reports (11–15).

Flow cytometric analysis of SAP

Flow cytometric analysis of SAP was performed as previously described (11, 12). The peripheral blood mononuclear cells (PBMC) were isolated by Ficoll–Hypaque density gradient centrifugation and immediately fixed in 1% paraformaldehyde for 30 min at room temperature and then permeabilized in 0.5% saponin for 15 min on ice. To test the expression of SAP in lymphocytes, these cells were incubated with 2 μg/ml anti-SAP mAb, termed KST-3 (rat IgG1) or irreverent rat IgG1, for 20 min on ice and further stained with a 1:1000 dilution of FITC-labeled goat anti-rat IgG antibody (Zymed, South San Francisco, CA, USA) or Alexa Fluor 488-conjugated goat anti-rat IgG antibody (Molecular Probes, Eugene, OR, USA) for 20 min on ice. To evaluate SAP expression in $CD8^+$ T and NK cells, PBMC were stained with phycoerythrin (PE)-conjugated anti-CD8 and anti-CD56 mAbs (DAKO Japan, Kyoto, Japan), respectively, before cellular fixation and permeabilization. The stained cells were analyzed using a flow cytometer (EPICS XL-MCL; Beckman Coulter KK, Tokyo, Japan).

SH2D1A mutation detection

The *SH2D1A* mutations were detected by direct sequencing as described previously (5, 14). Genomic DNA was purified from PBMC with a QIAamp Blood Kit (Qiagen, Hilden, Germany) and amplified using primers encompassing each exon–intron boundary of the *SH2D1A* genes. The sequencing reaction was carried out using a BigDye Terminator Cycle Sequencing Kit (Applied Biosystems, Foster City, CA, USA) with an automated ABI PRISM 310 DNA sequencer (Applied Biosystems).

Results

SAP expression in patients with XLP-1

Fresh blood cells were available in 19 patients with XLP-1. All the examined patients demonstrated markedly deficient SAP expression in lymphocytes, especially in $CD8^+$ T cells and NK cells (Fig. 1 and Table 1).

SH2D1A mutations

All the mutations including unpublished data are summarized with the clinical data (Table 1). There were three gross deletions (the whole gene and two exons 3 and 4), four nonsense mutations (all Arg55stop), eight missense mutations (Ala3Ser, Tyr7Cys, two His8Asp, Gly27Ser, Asp33Tyr, Ser34Gly and Gly49Val), two small deletions (584delA and 1021delAA), two small insertions (312insG and 545insA), and two splicing anomalies (416C>T and IVS2+1G>A). The substitution of 416C with T revealed an aberrantly spliced cDNA with deletion of the last 22 bases of exon 1, and IVS2+1G>A resulted in skipping of exon 2.

Clinical characteristics of Japanese patients with XLP-1

Eighteen of the 33 patients (55%) had FIM or EBV–HLH, 12 patients (36%) had hypogammaglobulinemia, seven patients (21%) had malignant lymphoma or lymphoproliferative disease, and two patients (P4.2 and P7.2) had lymphocytic vasculitis. One patient (P7.1) had aplastic anemia. Twenty-seven patients (82%) were associated with EBV infection at the disease onset. Two patients (P16.1 and P19.3) presented with non-EBV–HLH. Interestingly, malignant lymphoma and lymphocytic vasculitis in P4.2 were not associated with EBV infection, but the patient later developed EBV–HLH at the age of 14 yr and died of HLH. Two patients (P17.2 and P21.1) had encephalitis: and P17.2 developed acute disseminated encephalomyelitis caused by human